University of Milano-Bicocca and INFN

Performance of the CMS electromagnetic calorimeter and its role in the hunt for the Higgs boson in the two-gamma channel

Federico De Guio
on behalf of the CMS collaboration

International Workshop on Discovery Physics at the LHC
KRUGER 2012
December 3 - 7, 2012

The H→γγ search channel

- The H→γγ search channel played a crucial role in the discovery of a new resonance at a mass of 125 GeV
  - Small branching ratio, but very clear signature
  - Narrow resonance of two high E_T photons over a non-resonant background of genuine or fake di-photon events

- The discovery potential strongly depends on the invariant mass resolution
  - Energy resolution
  - Position/angle resolution
  - background rejection (π^0/γ separation)

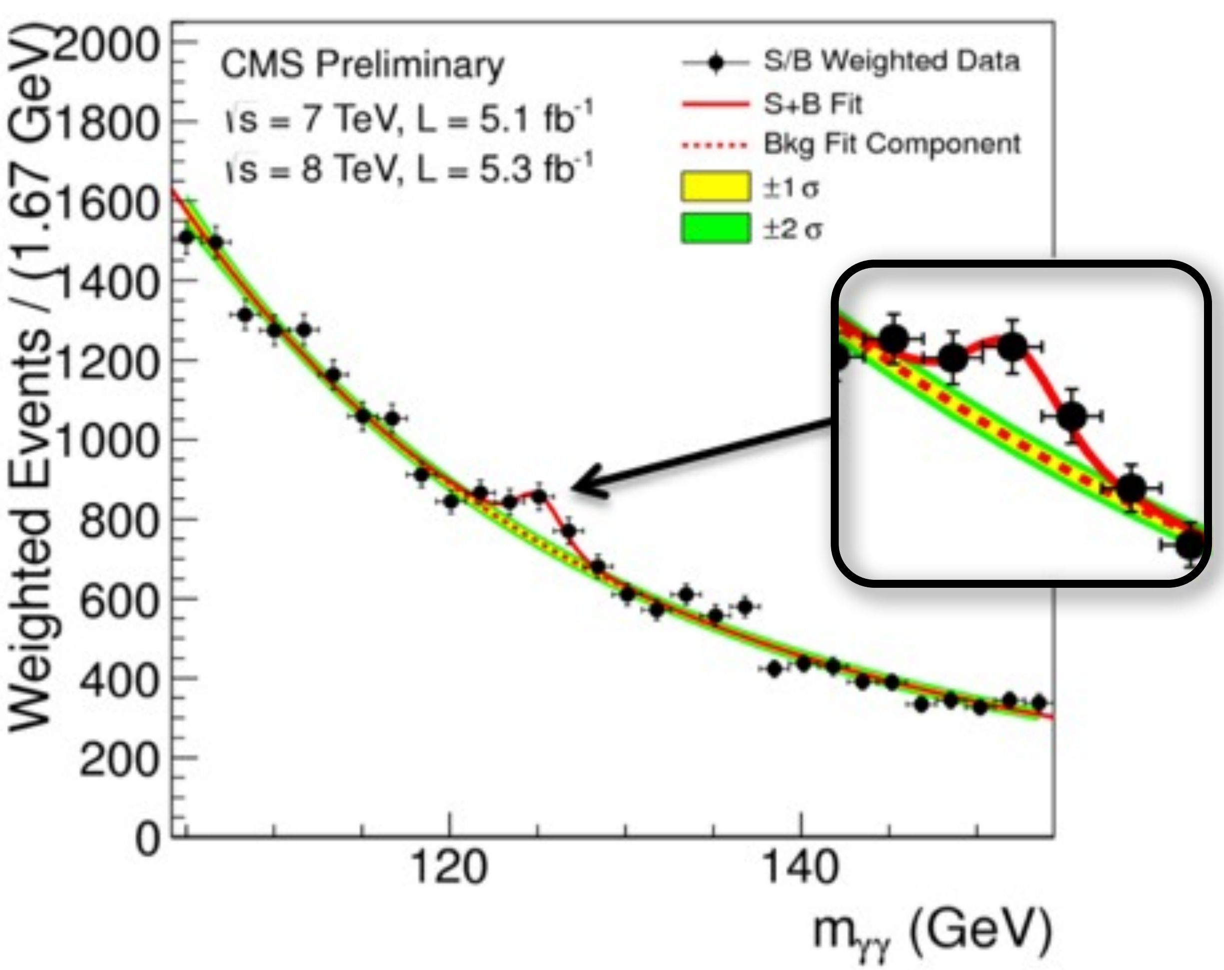

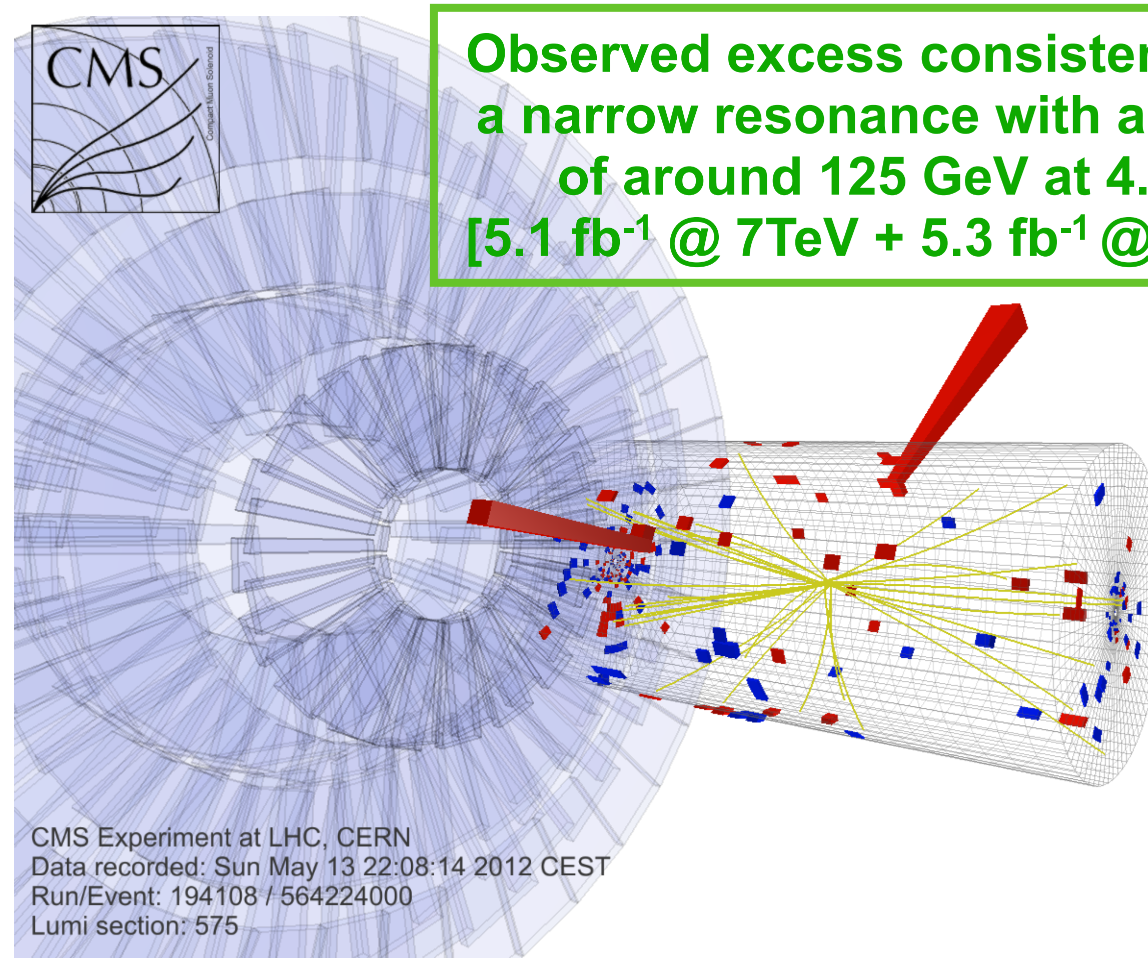

Observed excess consistent with a narrow resonance with a mass of around 125 GeV at 4.1σ [5.1 fb^{-1} @ 7TeV + 5.3 fb^{-1} @ 8TeV]

Outline

- The electromagnetic calorimeter of CMS (ECAL)
  - Description and performance
  - In-situ operation
- Energy calibration
  - e/γ energy measured with ECAL
  - Response stability and channel-to-channel calibration
  - Energy corrections
- Qualification of the performance with Z→ee events
  - Measurement of the energy scale and resolution
- Impact of the performance on the H→γγ signal
  - Progress in understanding ECAL
- Summary

The CMS ECAL

- ECAL is a **homogeneous, compact, hermetic, fine grain** scintillating calorimeter composed of 75848 **lead tungstate crystals** ($PbWO_4$) organized in barrel (EB) and endcaps (EE)
- Excellent energy resolution for photons and electrons **(H→γγ, H→ZZ →4e)**

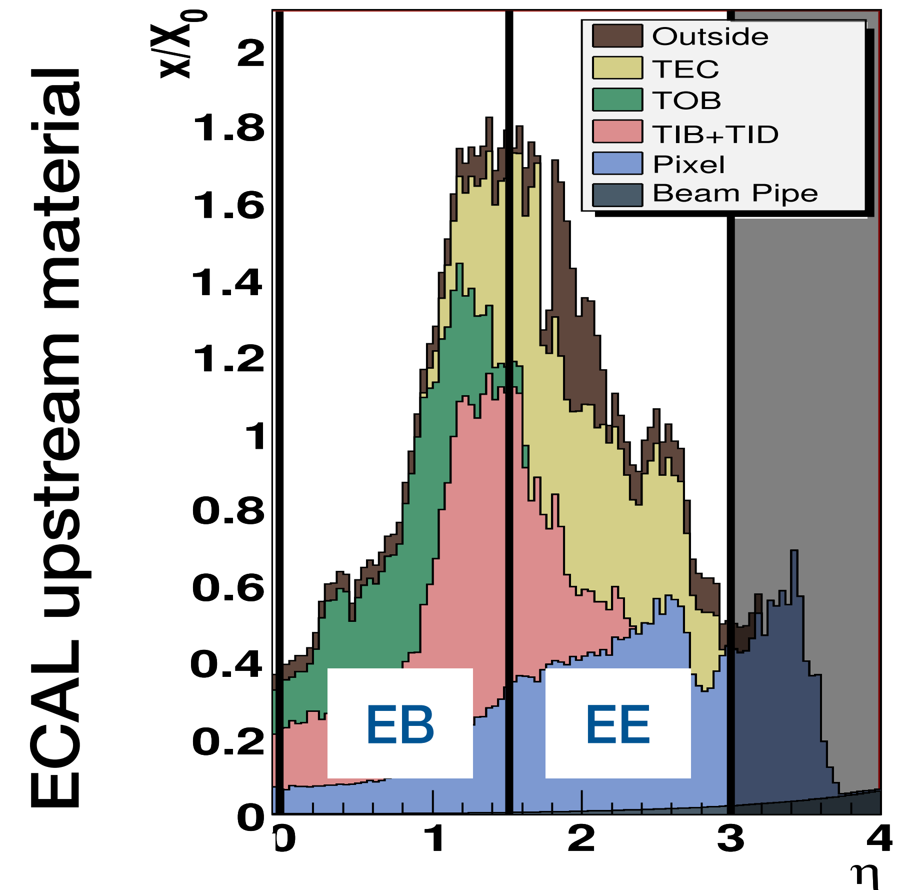

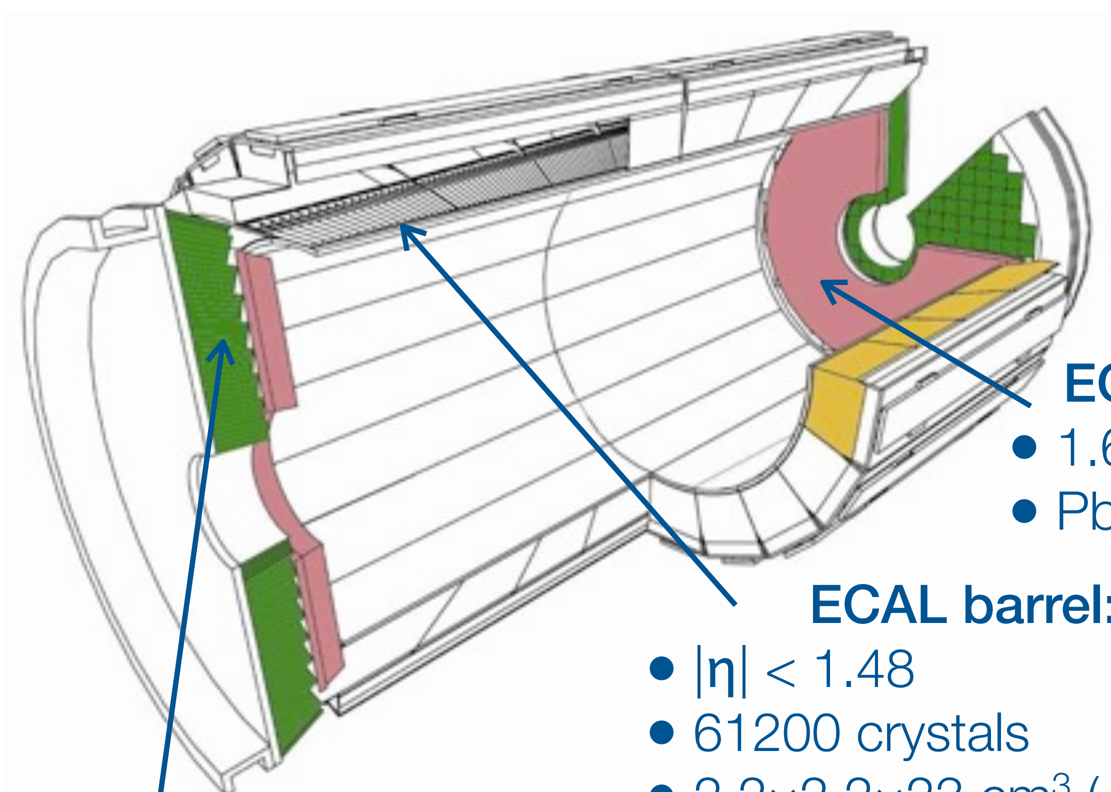

ECAL preshower:
- $1.65 < |\eta| < 2.60$
- Pb/Si (~$3X_0$)

ECAL barrel:
- $|\eta| < 1.48$
- 61200 crystals
- $2.2\times2.2\times23$ cm^3 (~$26X_0$)

ECAL endcap:
- $1.48 < |\eta| < 3.00$
- 14648 crystals
- $3\times3\times22$ cm^3 (~$25X_0$)

- ~4.5 photo-electrons/MeV
- high density (8.9 g/cm^3)
- small Molière radius (2.19 cm)
- short rad. length (0.89 cm)
- Transparency variation with radiation [measured and corrected]
- **excellent energy resolution [0.5% at high energies]**

Response spread → Intercalibration
Response stability → Stabilization and monitoring

Energy resolution and performance

- ECAL 'standalone' energy resolution measured at **test beams** (120 GeV electrons)
  - No magnetic field, no material upstream of ECAL
  - Negligible systematic term from channel response variations (inter-calibration)
- Energy resolution for central impact on 3x3 arrays of barrel crystals

$$\frac{\sigma_E}{E} = \frac{2.8\%}{\sqrt{E(GeV)}} \oplus \frac{0.128}{E(GeV)} \oplus 0.3\%$$

Stochastic term (A)
Noise term (B)
Constant term (C)

- Results used to tune MC simulation

- **At high energy, the photon resolution is dominated by the constant term C**
- Additional contribution to the energy resolution in CMS:
  - **Environmental stability and response uniformity**
  - **The target is to keep C ~ 0.5%**

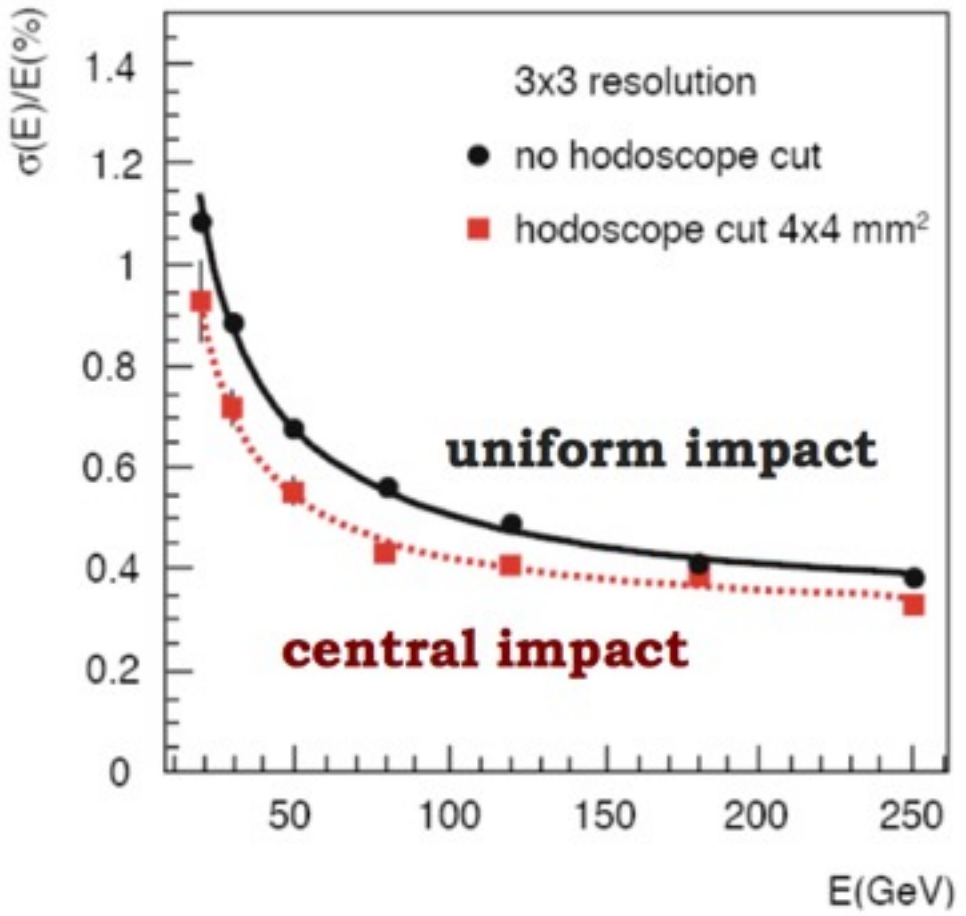

In-situ operation

- **ECAL stably and efficiently running**
  - Fraction of working channels stable in the last three years: **EB 99.2%, EE 98.5%, ES 96.9%**
  - Temperature stability:
    - negligible contribution to the energy resolution constant term if temperature of the Barrel/Endcap stable **within 0.05 °C/0.1 °C**
  - High Voltage stability (EB):
    - APD gain very sensitive to the bias voltage: 3%/Volt
    - High Voltage stability: **~0.1% contribution to the C term**

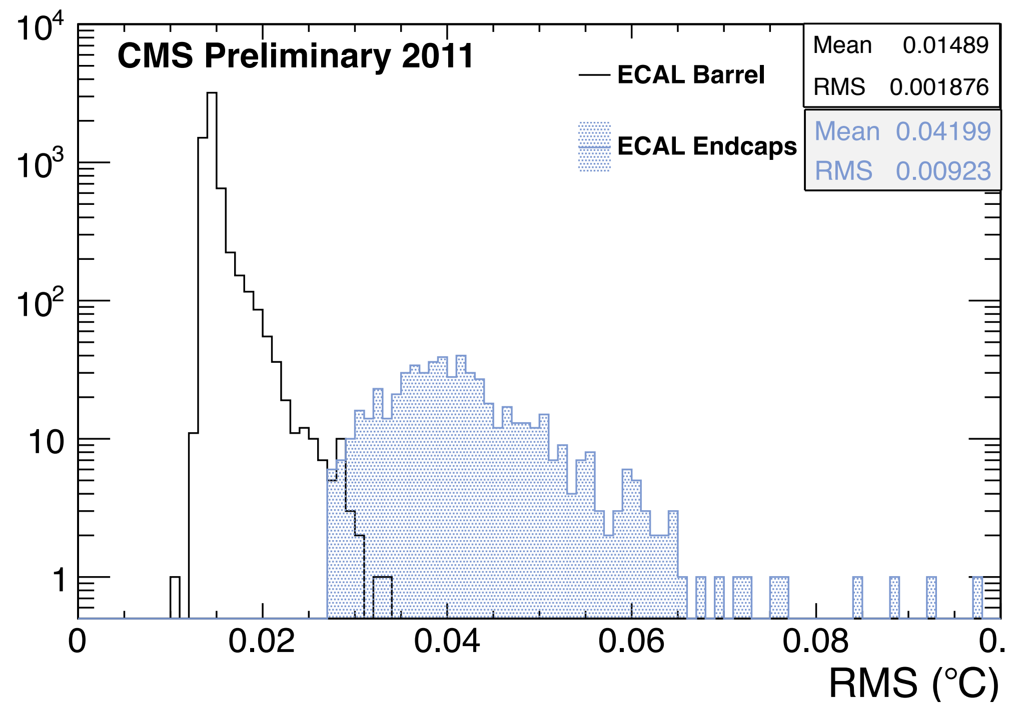

- **Excellent triggering efficiency** (Level-1 e/γ trigger with 15 GeV E_T threshold)
  - Efficiency estimate with the tag and probe method from the Z→ee decay
    - **at 100 GeV: 99.95% in EB and 99.84% in EE**
  - Response corrections applied at trigger level since the beginning of the 2012 run

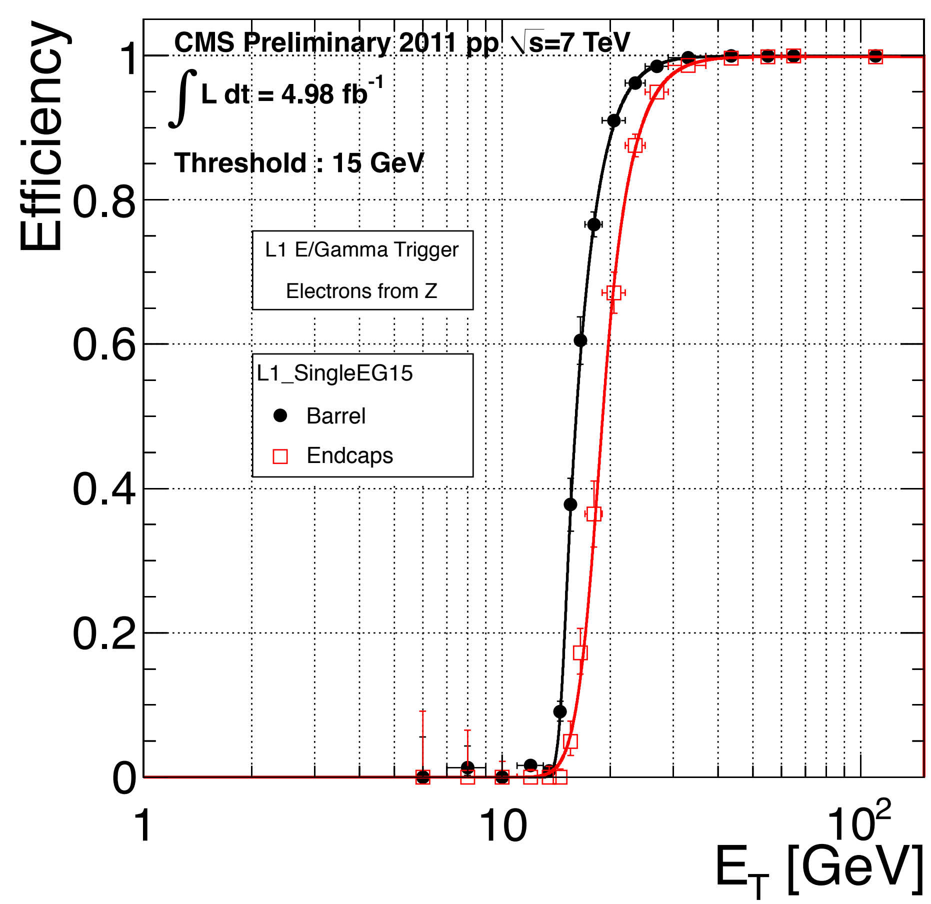

- **Removal of anomalous signals** already at trigger level
  - consisting of isolated large signals coming from the direct ionization of the active silicon layers of the APDs

ECAL energy calibration

- In-situ calibration to get the **best estimate of the energy of e/γ**
- Energy spread over several crystals ⇒

$$E_{e/\gamma} = F_{e/\gamma} \cdot G \cdot \Sigma_i \left[S_i(t) \cdot c_i \cdot A_i \right]$$

- A_i: single channel amplitude (ADC counts)
- c_i: inter-calibration constant
- $S_i(t)$: time-dependent correction for response variations
- G: global scale calibration (GeV/ADC)
- $F_{e/\gamma}$: particle energy correction (geometry, clustering, ...)

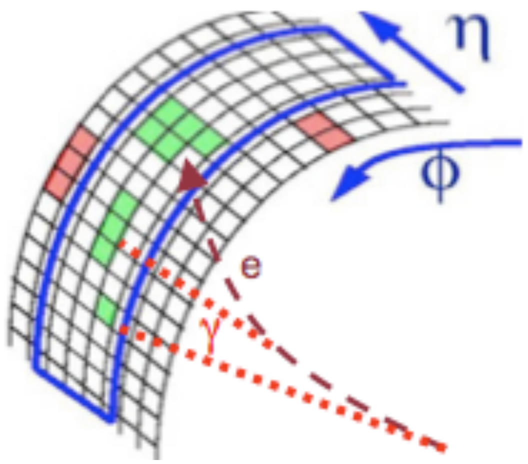

- The intercalibration [c_i] and the response stability [$S_i(t)$] precision **directly affect the constant term C**
- **In-situ calibration and monitoring** sources with collision events
  - **$\pi^0/\eta \rightarrow \gamma\gamma$ mass**
  - **φ- and time-invariance of the energy flow** per crystal in Minimum bias events
  - **Electron E/p and Z→ee mass**

  } **Dedicated high-rate calibration data streams**
- **Energy scale and resolution** (and efficiency and particle id)
  - **Z→ee and Z→μμγ**

ECAL response variation with irradiation

- The $PbWO_4$ **scintillation mechanism** is **not affected** by irradiation. But irradiation causes:
  - **variations in crystal transparency**
  - **VPT ageing**

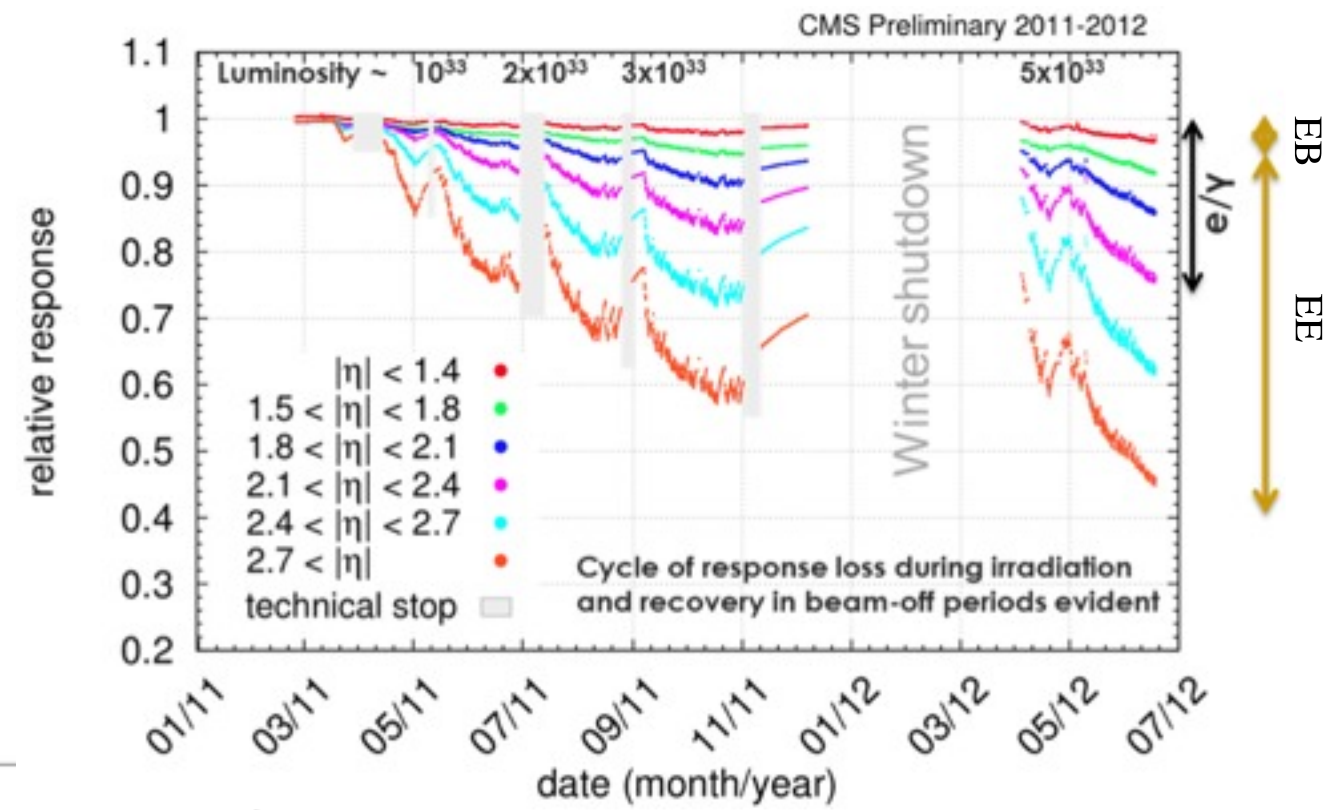

- Response monitored with laser light at 440 nm (close to max. scintillation emission) and 798 nm

- Crystal response to laser and e.m. shower light linked by $S/S_0 = (R/R_0)^{\alpha}$

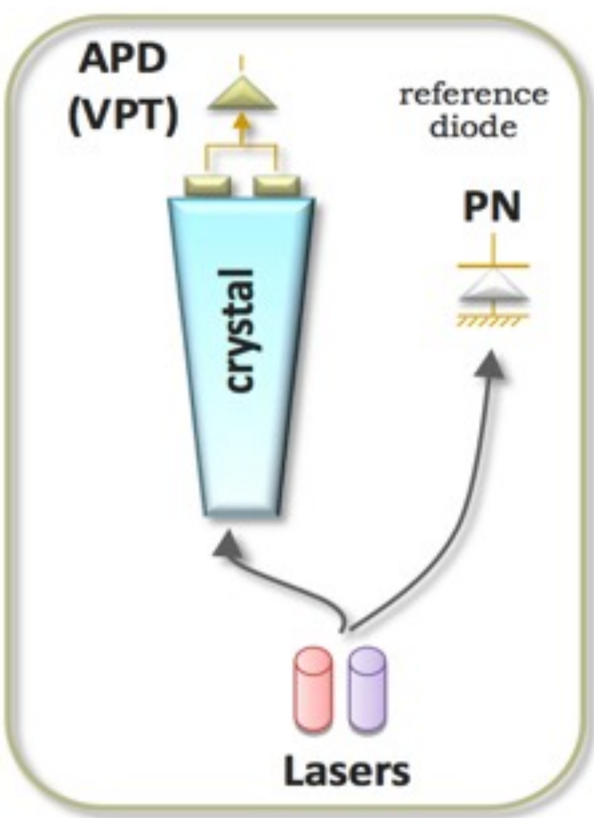

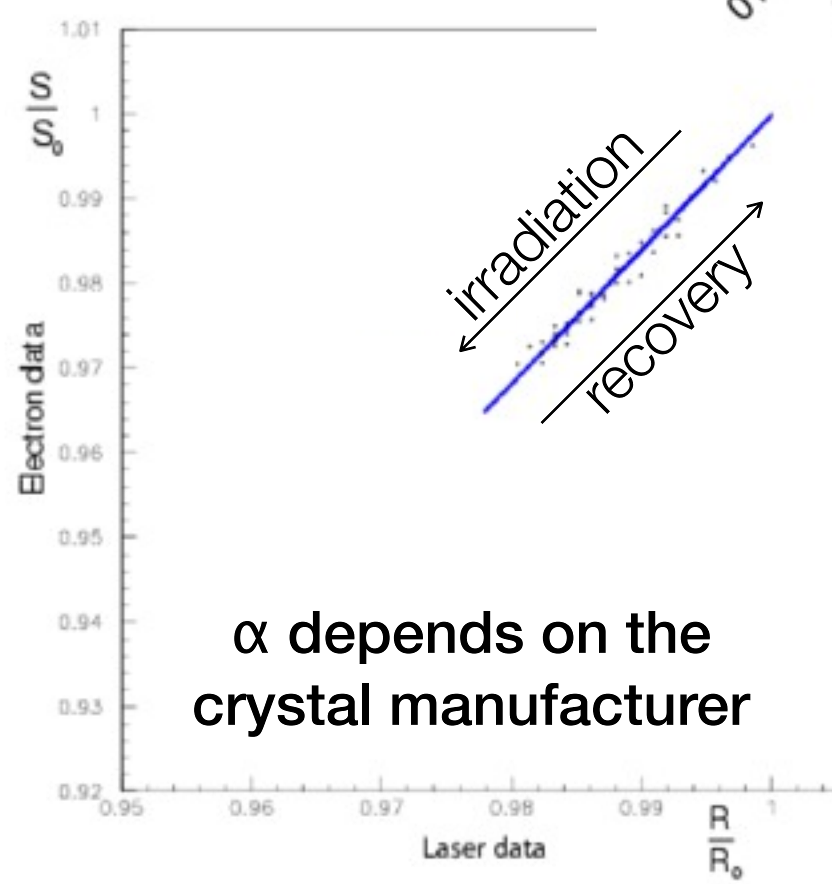

α depends on the crystal manufacturer

- creation of **colour centers** which absorb the scintillation light
- **rapid loss and recovery** of the optical transmission under irradiation (few hours)
- LHC cycles clearly visible

$$E_{e/\gamma} = F_{e/\gamma} \cdot G \cdot \Sigma_i \left[S_i(t) \cdot c_i \cdot A_i \right]$$

Monitoring the stability of the response vs time

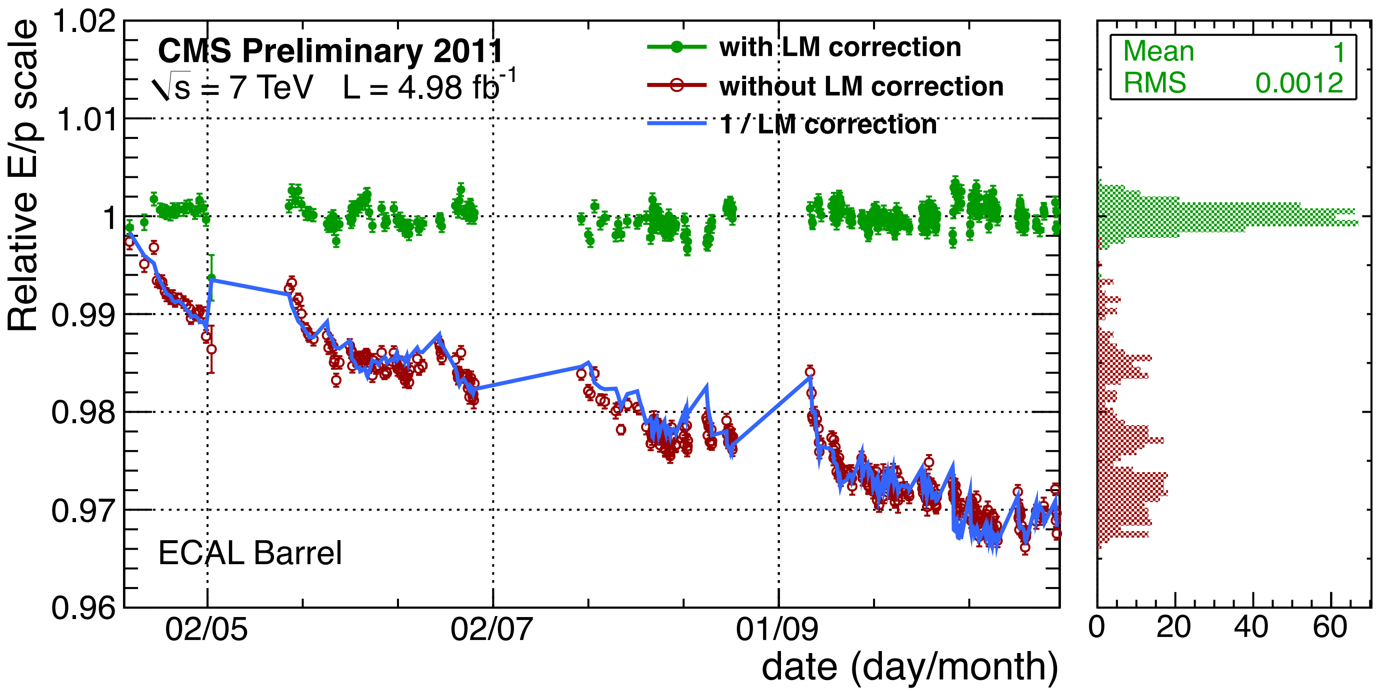

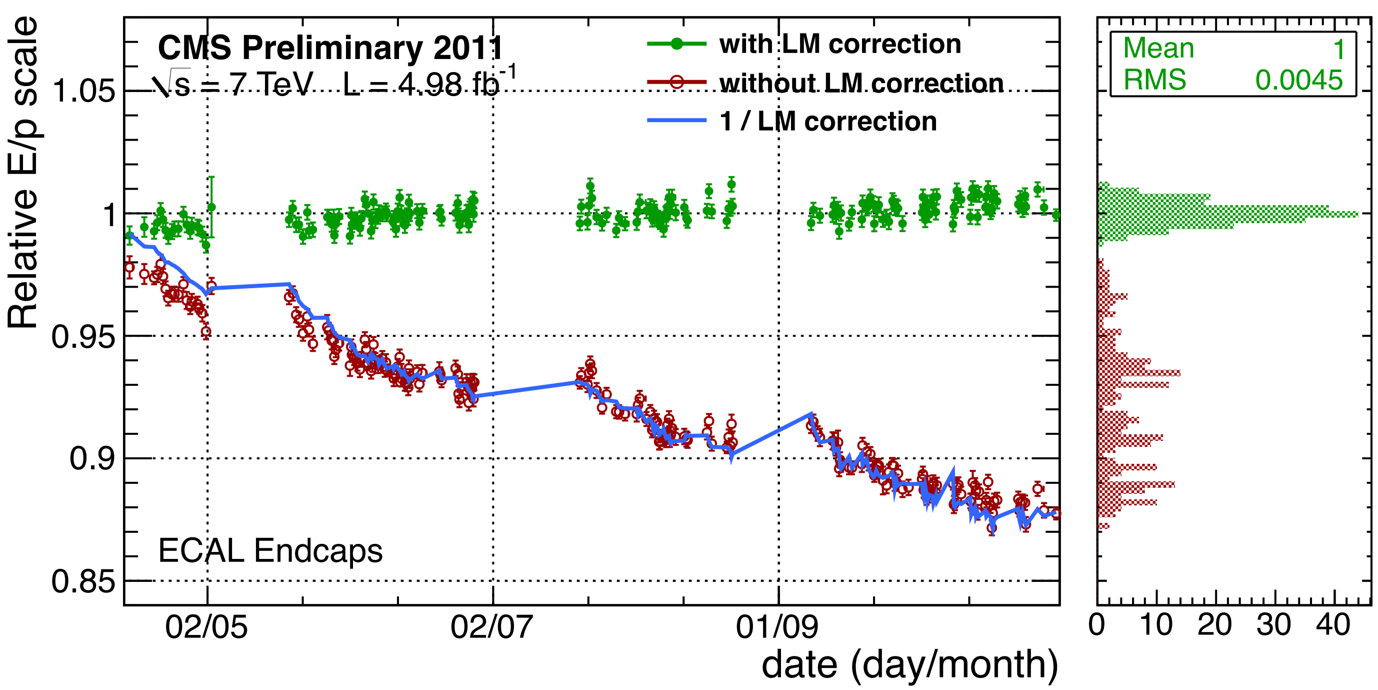

- **Stable energy scale after correcting for response changes.**
- Barrel:
  - <signal loss> ~ 2.5%,
  - RMS stability ~0.12%
- Endcap:
  - <signal loss> ~10%,
  - RMS stability ~0.45%
- Corrections include:
  - Barrel: $\alpha = 1.52$
  - Endcap: $\langle\alpha\rangle \sim 1.28$
- Further tuning of the corrections in progress:
  - Residual effective corrections from E/p and π^0 history

$$E_{e/\gamma} = F_{e/\gamma} \cdot G \cdot \Sigma_i \left[S_i(t) \cdot c_i \cdot A_i \right]$$

Monitoring the stability of the response vs time

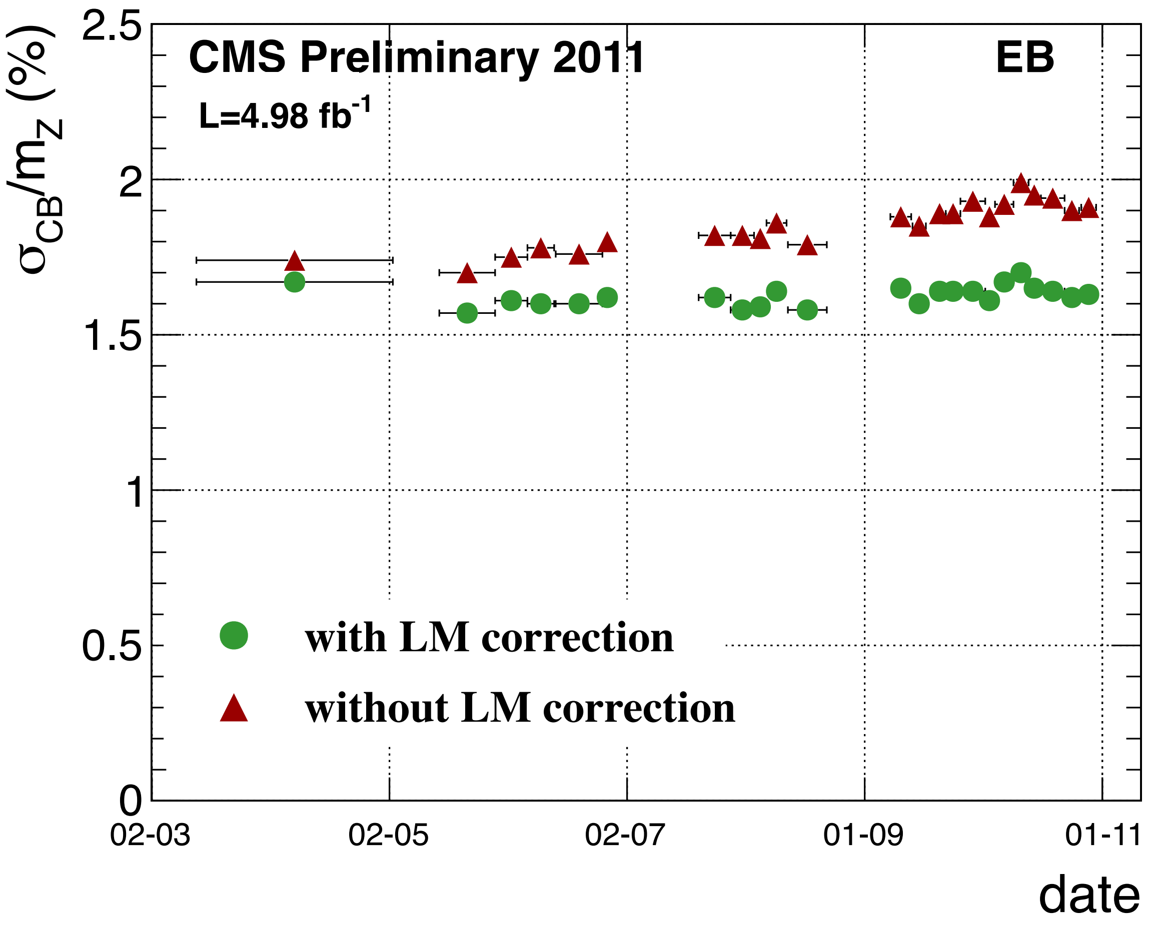

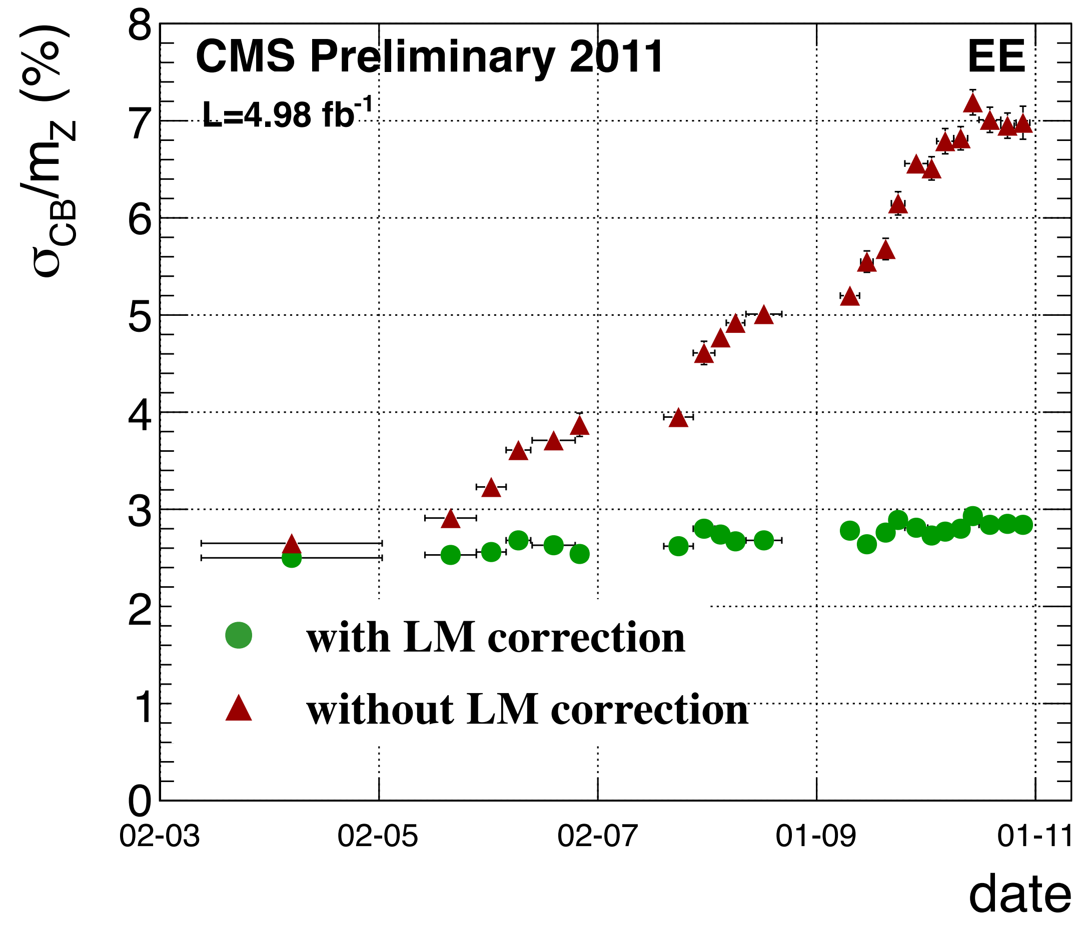

- ECAL resolution (from **Z→ee peak width**) stability before and after the application of Laser Monitoring corrections (LM):
  - ECAL Barrel: resolution stable within errors
  - ECAL Endcaps: resolution worsens by ~1.5% in quadrature
- Further tuning of corrections and/or pileup effects is required
  - e.g. in-situ measurement of the 'effective α' at single crystal level

$$E_{e/\gamma} = F_{e/\gamma} \cdot G \cdot \Sigma_i \left[S_i(t) \cdot c_i \cdot A_i \right]$$

Single channel inter-calibration

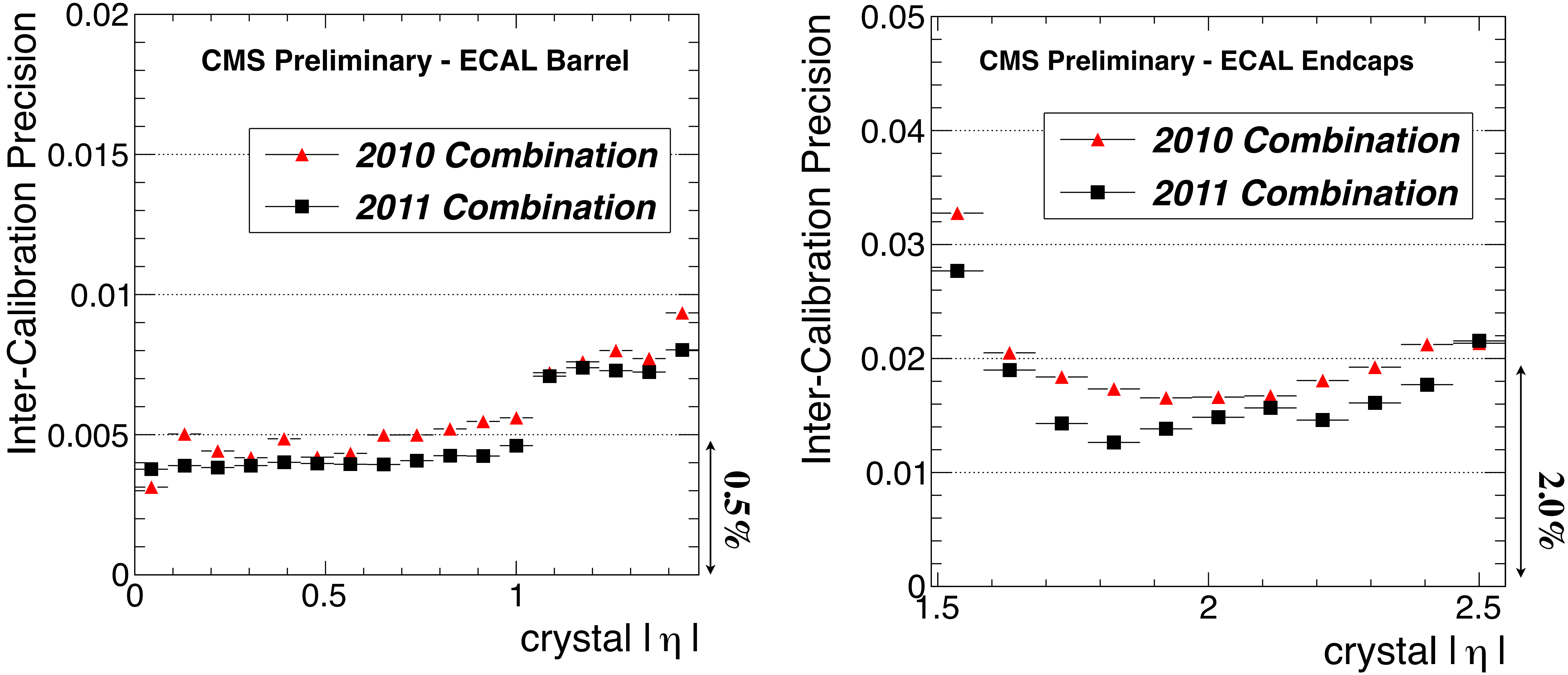

- Several methods to calibrate in-situ:
  - **φ-symmetry calibration:** invariance around the beam axis of energy flow in minimum bias events. Intercalibrate crystals at the same pseudorapidity.
  - **π^0 and η calibration:** mass constraint on photon energy, use unconverted γ's reconstructed in 3x3 matrices of crystals.
  - **High energy electron** from W and Z decays (E/p with single electrons and invariant mass with double electrons).

$$E_{e/\gamma} = F_{e/\gamma} \cdot G \cdot \Sigma_i \, [\, S_i(t) \cdot c_i \cdot A_i \,]$$

Impact of the calibration on the Z→ee peak

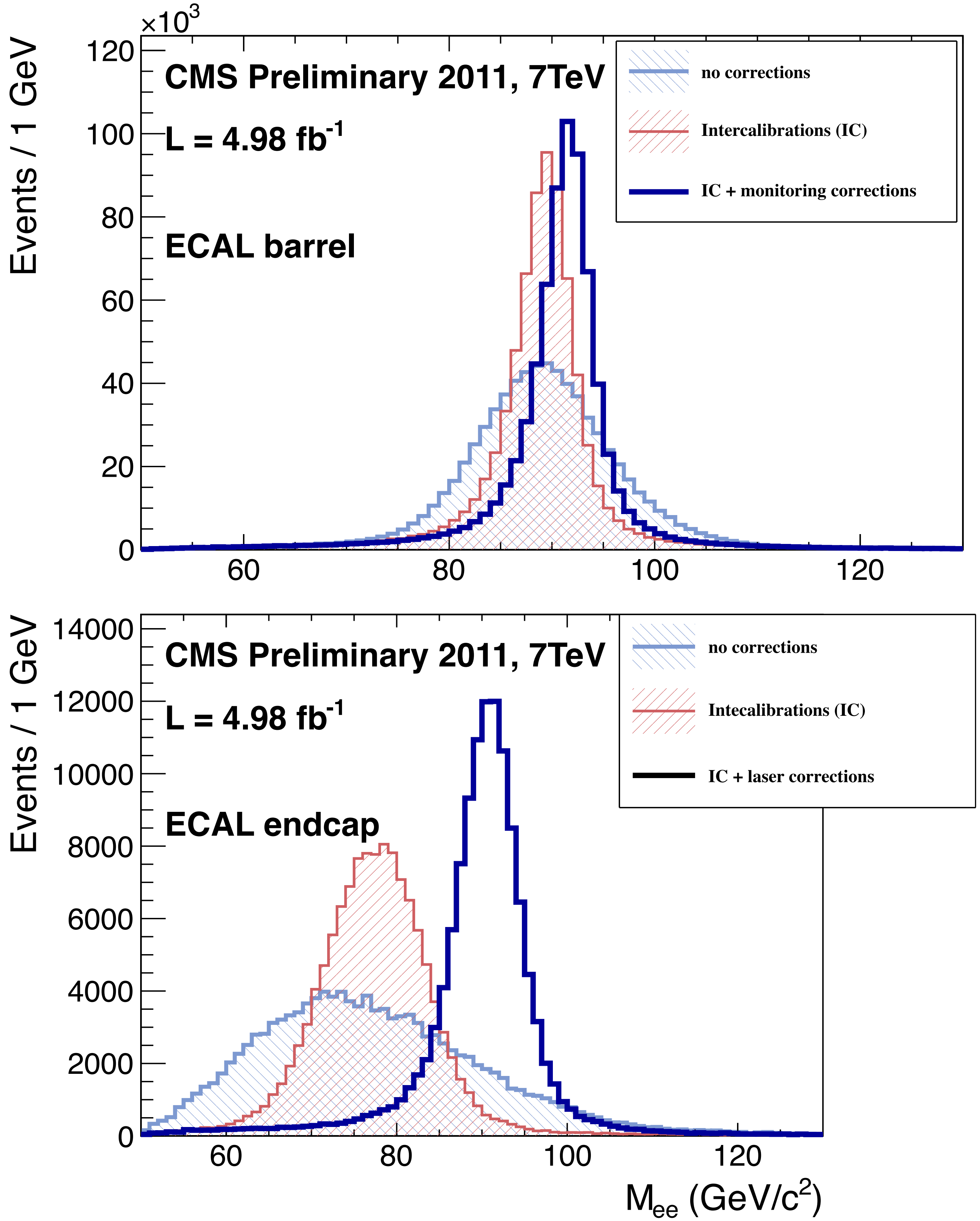

- Impact on the reconstructed **di-electron invariant mass** of:
  - inter-calibration coefficients
  - inter-calibration + laser corrections

- The three inter-calibration methods are approaching the **asymptotic precision** in EB
  - The estimate of the IC and their precision is in agreement in 2010, 11 and 12 data
  - Some improvement can be obtained trying to correct for time instabilities

- On top of the single channel calibration, **e/γ dependent algorithmic corrections** based on simulation (MC) are applied.

$$E_{e/\gamma} = F_{e/\gamma} \cdot G \cdot \Sigma_i \left[S_i(t) \cdot c_i \cdot A_i \right]$$

Energy corrections

- **Cluster energy corrections** vs pseudo-rapidity for non-showering and showering electrons:
  - compensate for unclustered energy and energy not reaching the calorimeter: **strongly related to the amount of material in front of ECAL**.
  - energy lost inside gaps: intermodule boundary visible in the Barrel
- Current best corrections from an **MC driven MVA analysis** including shower location, shower-shape, and global event variables

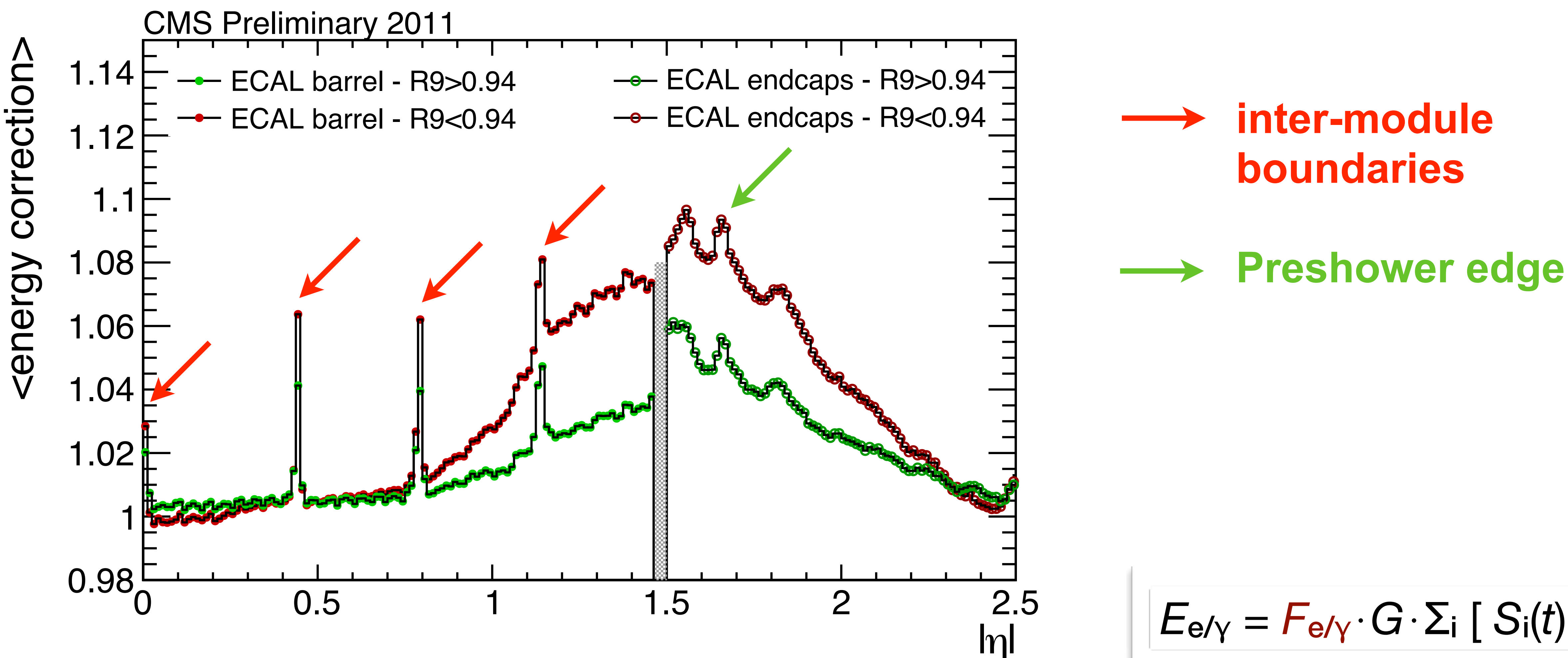

$$E_{e/\gamma} = F_{e/\gamma} \cdot G \cdot \Sigma_i \left[S_i(t) \cdot c_i \cdot A_i \right]$$

Energy corrections

- Studied **E/p vs η**
  - **ad-hoc p calibration** obtained from $Z \rightarrow ee$ events applied
  - fit each η ring with a template distribution
  - MC is flat ⇔ $F_{e/\gamma}$ well tuned
  - **data/MC difference used to adjust the scale along η**

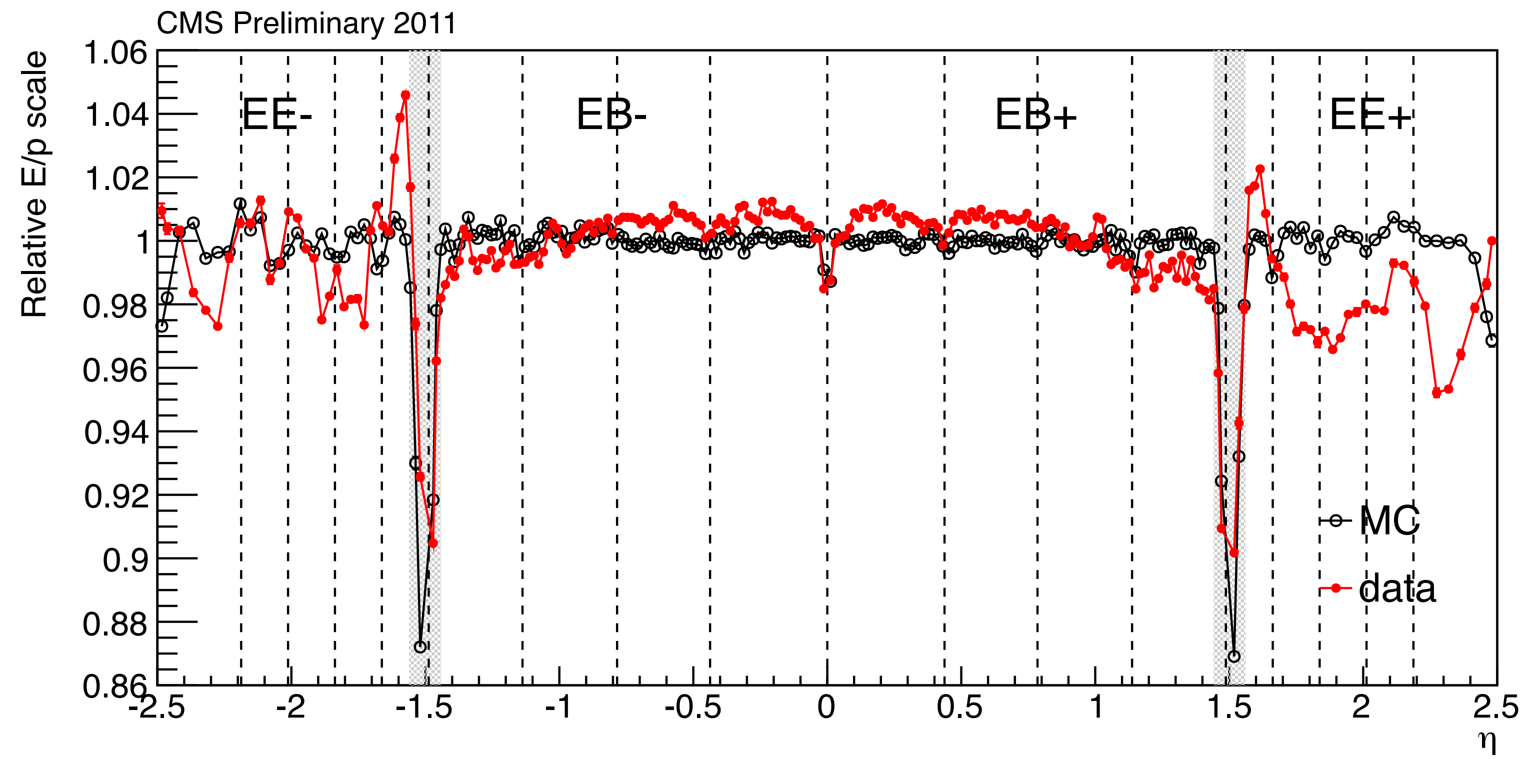

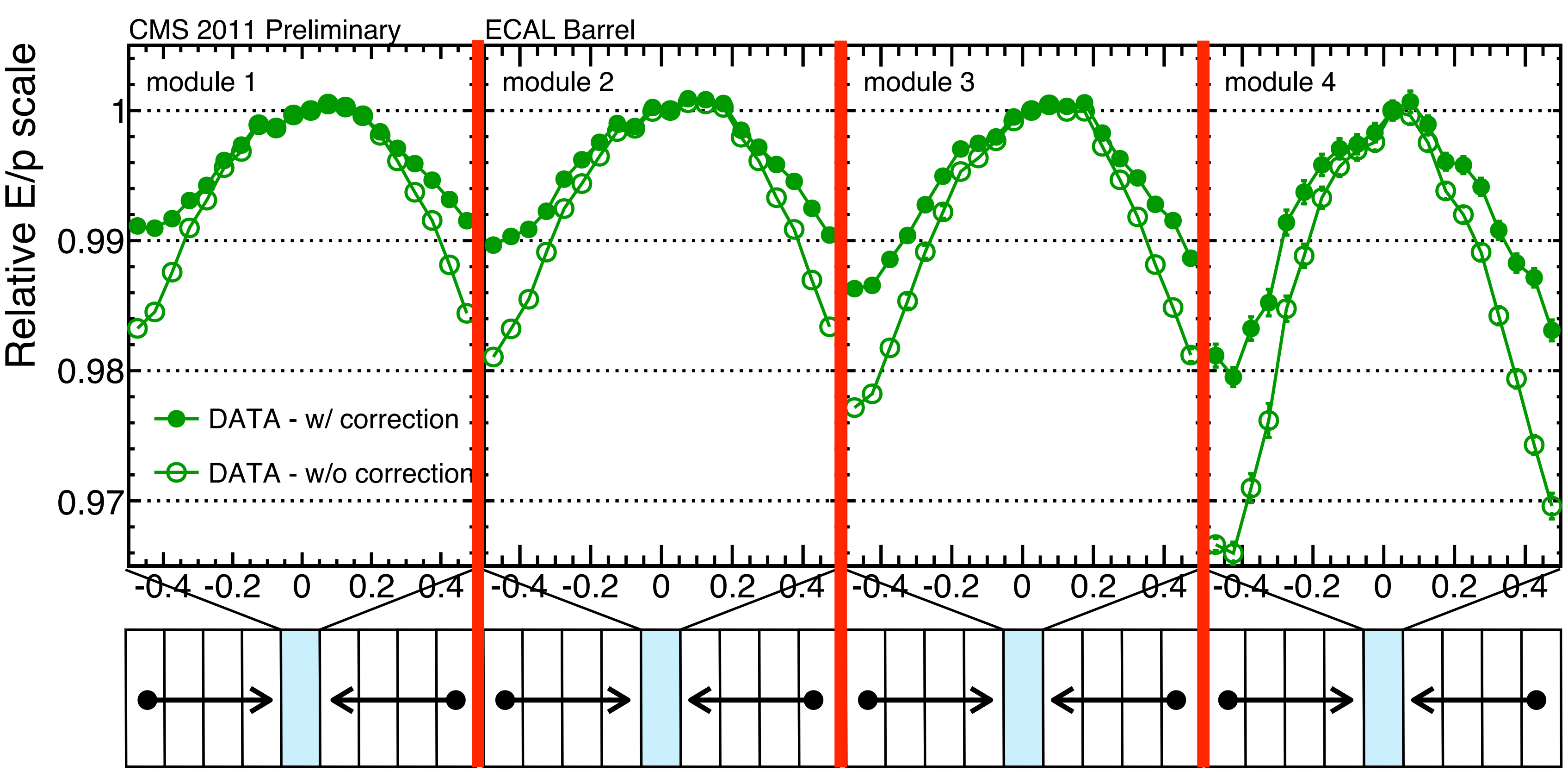

- Studied **E/p vs local η**
  - all ECAL folded in 1 crystal - four η regions defined
  - residual dependence on the electron impact position observed

$$E_{e/\gamma} = F_{e/\gamma} \cdot G \cdot \Sigma_i \, [\, S_i(t) \cdot c_i \cdot A_i \,]$$

Energy and mass resolution

- The **Z→ee invariant mass peak** is the main tool to estimate energy resolution and scale.
- The Z→ee events are fitted with the **convolution of a Breit-Wigner and a Crystal-Ball** function.
- An extra-smearing is applied to the simulation in order to match the energy resolution measured in the data

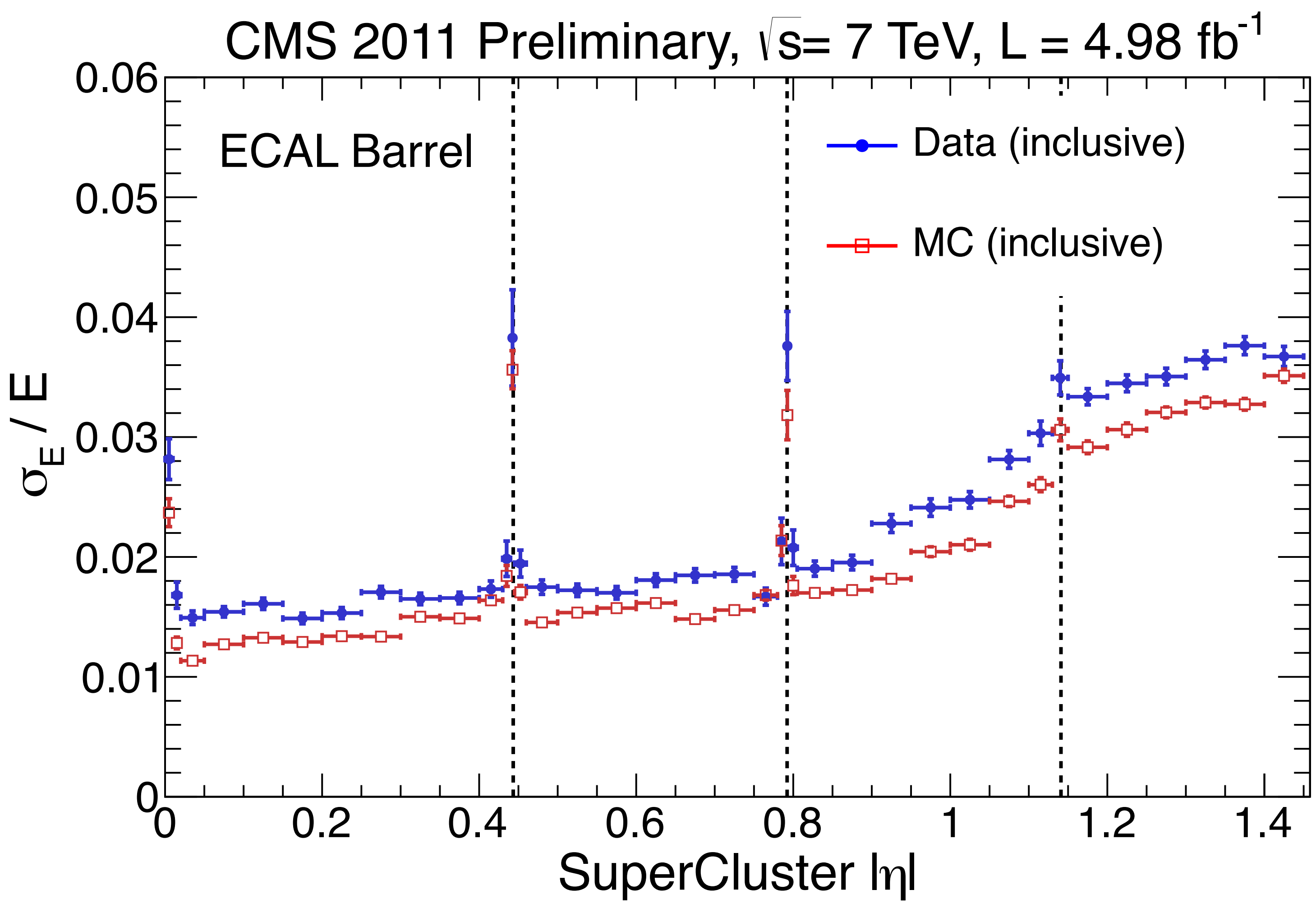

- **Energy scale:**
  - consistent with PDG within 0.6% syst.
- **Energy resolution:**
  - 1.01 GeV/c^2 for low bremsstrahlung
  - 1.56 GeV/c^2 inclusive category

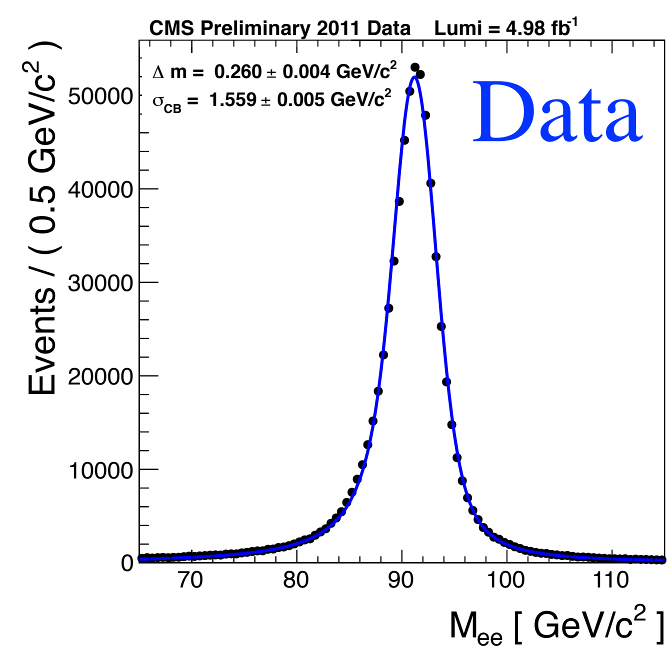

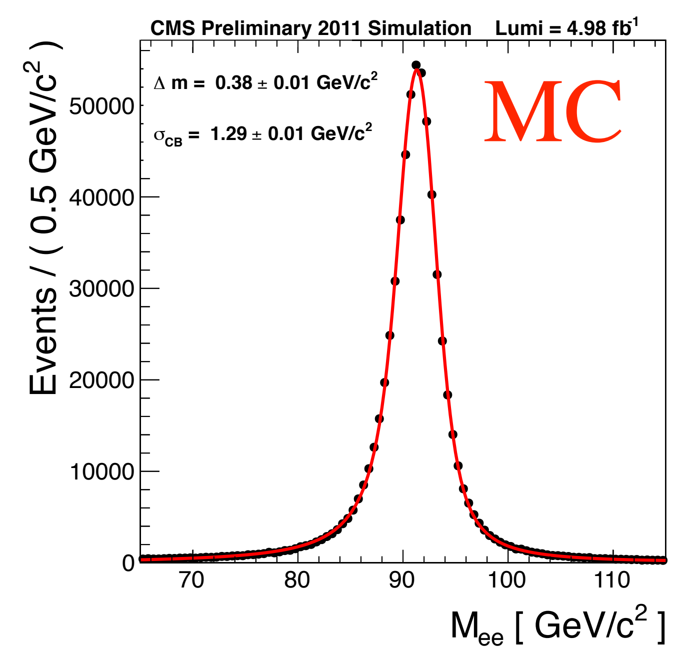

Energy and mass resolution

- **Room for improvement in EE**
  - reduce the inter-calibration systematic effects
  - optimization of cluster corrections

- Tuning of the simulation in order to **reduce the data-MC discrepancy:**
  - single crystal response description
  - energy and geometry corrections
  - tracker material description

- **Consistent results from Z→μμγ** both in barrel and in endcap

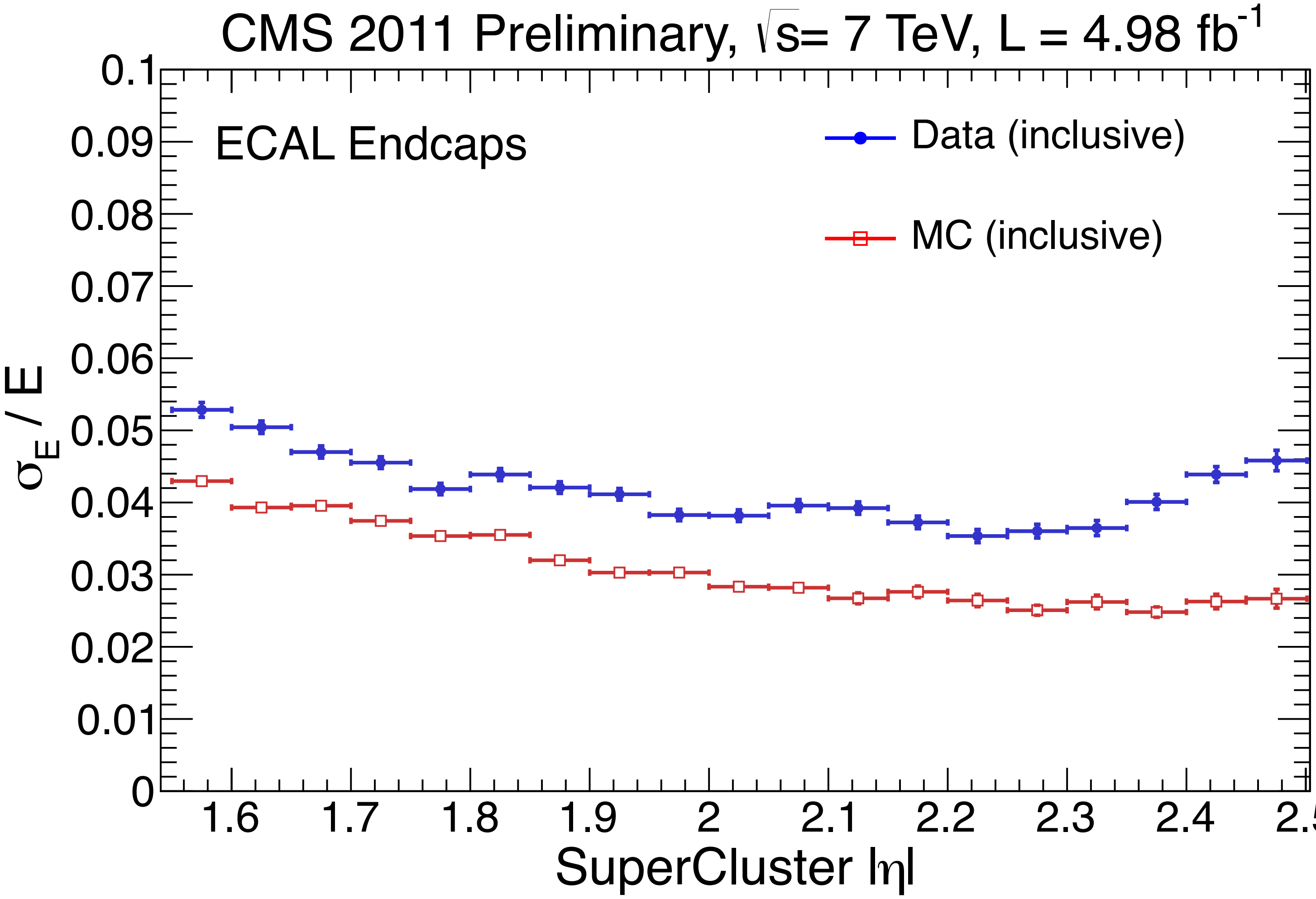

- **Energy scale:**
  - consistent with PDG within 1.5% syst.
- **Energy resolution:**
  - 2.57 GeV/c^2 for inclusive category

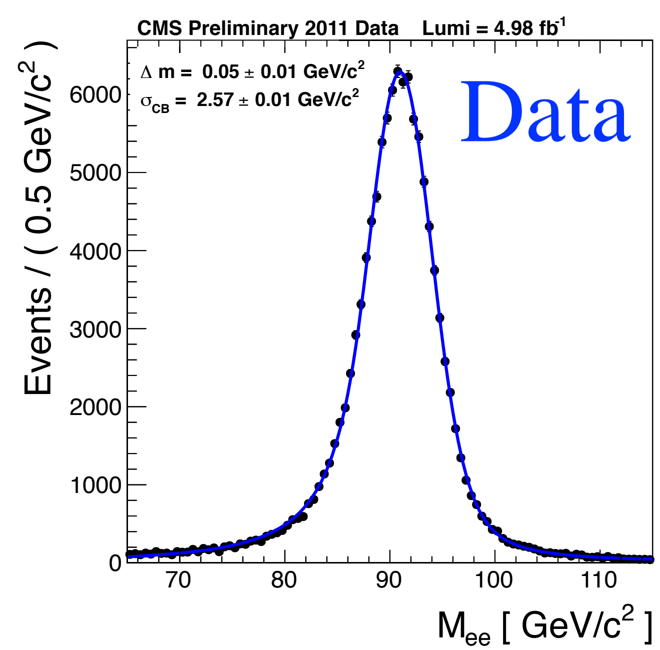

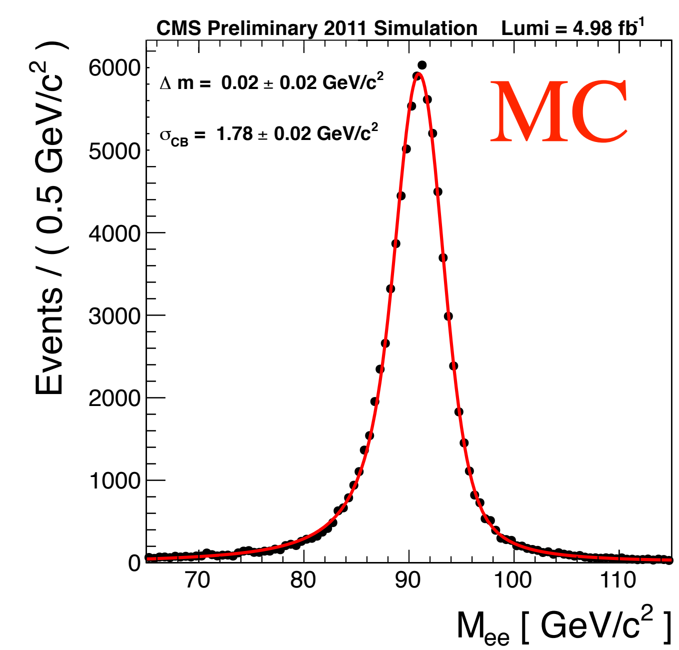

Impact of the performance on the H→γγ signal

- All the improvements in the **understanding of the ECAL** energy reconstruction and corrections contribute significantly to enhance the **H→γγ discovery potential**
- Inclusive H→γγ invariant mass distribution after the MC energy smearing
- Golden category (unconverted photons in EB): **FWHM/2.35 = 1.04 GeV (0.87%)**

July 2011 EPS **re-reco**	March 2012 Moriond **re-reco**	**Used to set the limit** July 2012 ICHEP **prompt-reco**	July 2012 ICHEP **re-reco**
FWHM/2.35 = 1.80GeV (1.50%)	**FWHM/2.35 = 1.40GeV (1.17%)**	**FWHM/2.35 = 1.57GeV (1.31%)**	**FWHM/2.35 = 1.35GeV (1.13%)**

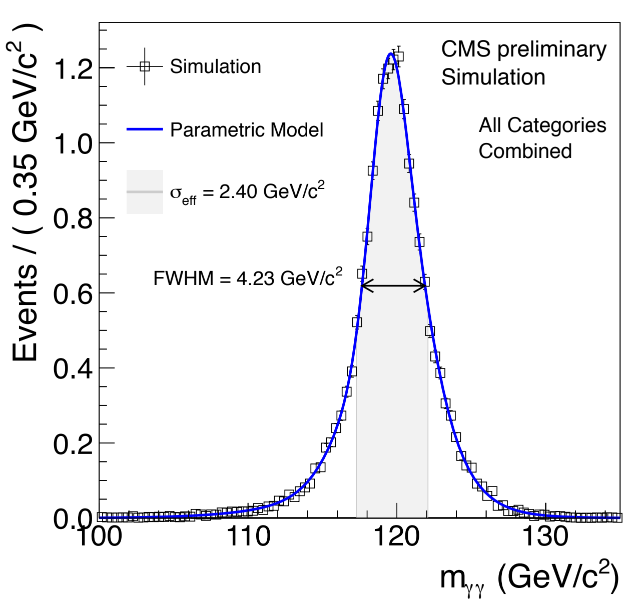

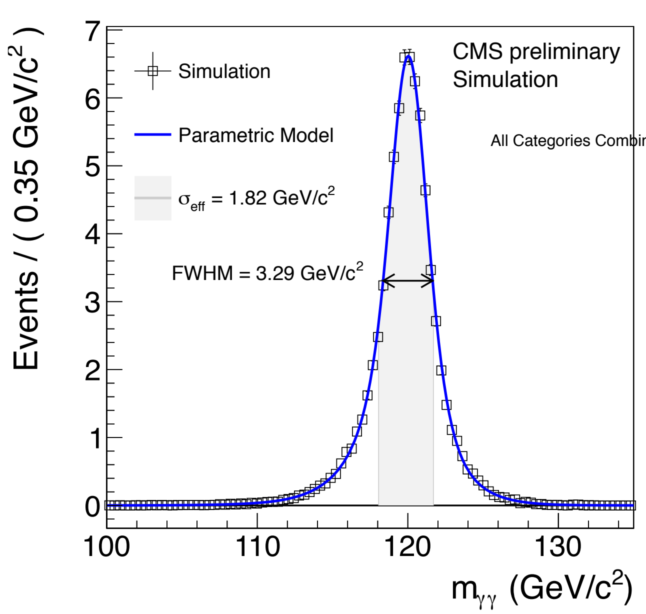

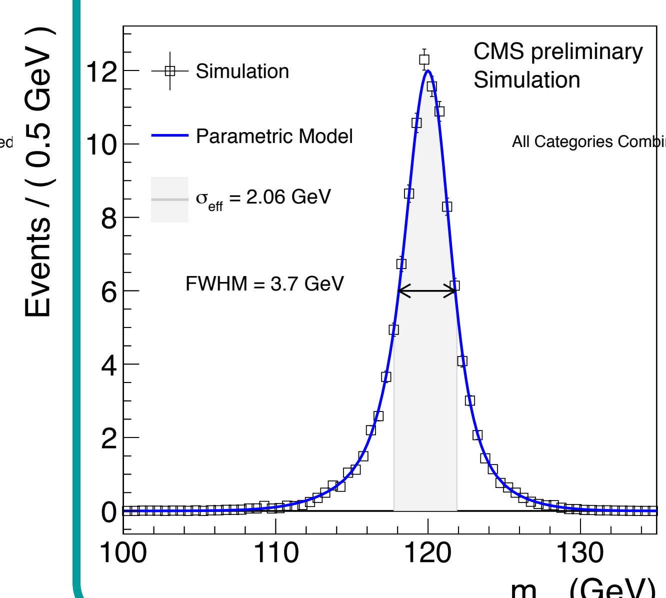

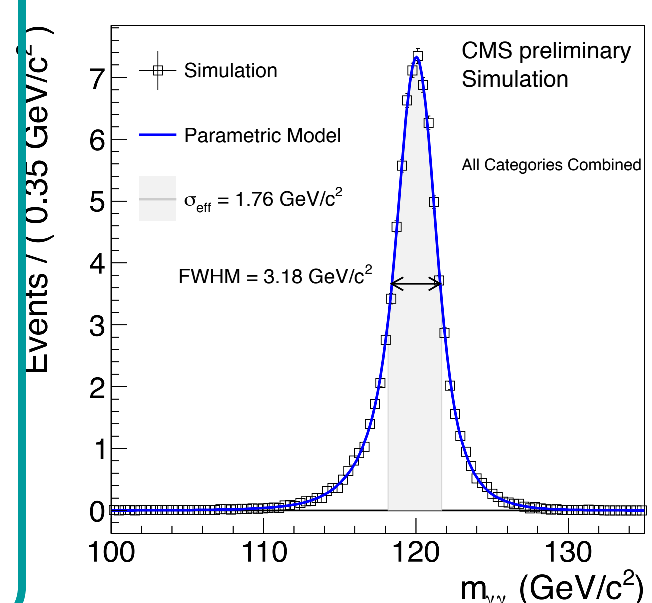

Summary

- Stable and efficient running during 2011 and 2012 data taking
  - Negligible impact on the energy resolution from the operation of the cooling and high voltage
  - Data taking efficiency: > 97.5% for ECAL, nearly 100% for the preshower

- Excellent performance
  - Decisive contribution to the discovery of a new resonance with a mass of 125 GeV
  - Mass resolution of 125 GeV Higgs boson decaying to two photons: 0.87% achieved for golden category in the barrel

- Still room for improvement in the endcaps (less contributing to the $H \to \gamma\gamma$ sensitivity with respect to the barrel)
  - tuning of the inter-calibration and energy correction to the data
  - tracker material description in simulation

References

- CMS Coll., ECAL 2011 performance results, CMS-DP-2012-007 and CMS-DP-2012-008 (2012)
- CMS Coll., Electromagnetic calorimeter calibration with 7 TeV data, CMS- PAS-EGM-2010-003 (2010)
- CMS Coll., Electromagnetic calorimeter commissioning and first results with 7 TeV data, CMS NOTE-2010/012 (2010)
- CMS coll., Performance and operation of the CMS electromagnetic calorimeter, J.Inst. 5 T03010 (2010)
- P.Adzic et al. (CMS ECAL), Intercalibration of the barrel electromagnetic calorimeter of the CMS experiment at start-up, J.Inst. 3 P10007 (2008)
- P.Adzic et al. (CMS ECAL), Energy resolution of the barrel of the CMS Electromagnetic Calorimeter, J.Inst. 2 P04004 (2007)
- M. Anfreville et al., Laser monitoring system for the CMS lead tungstate crystal calorimeter, NIM A594 (2008) 292-320
- CMS coll., Physics Tech. Design Report, Vol. I, CERN-LHCC-2006-001 (2006) CERN

Backup

The Compact Muon Solenoid

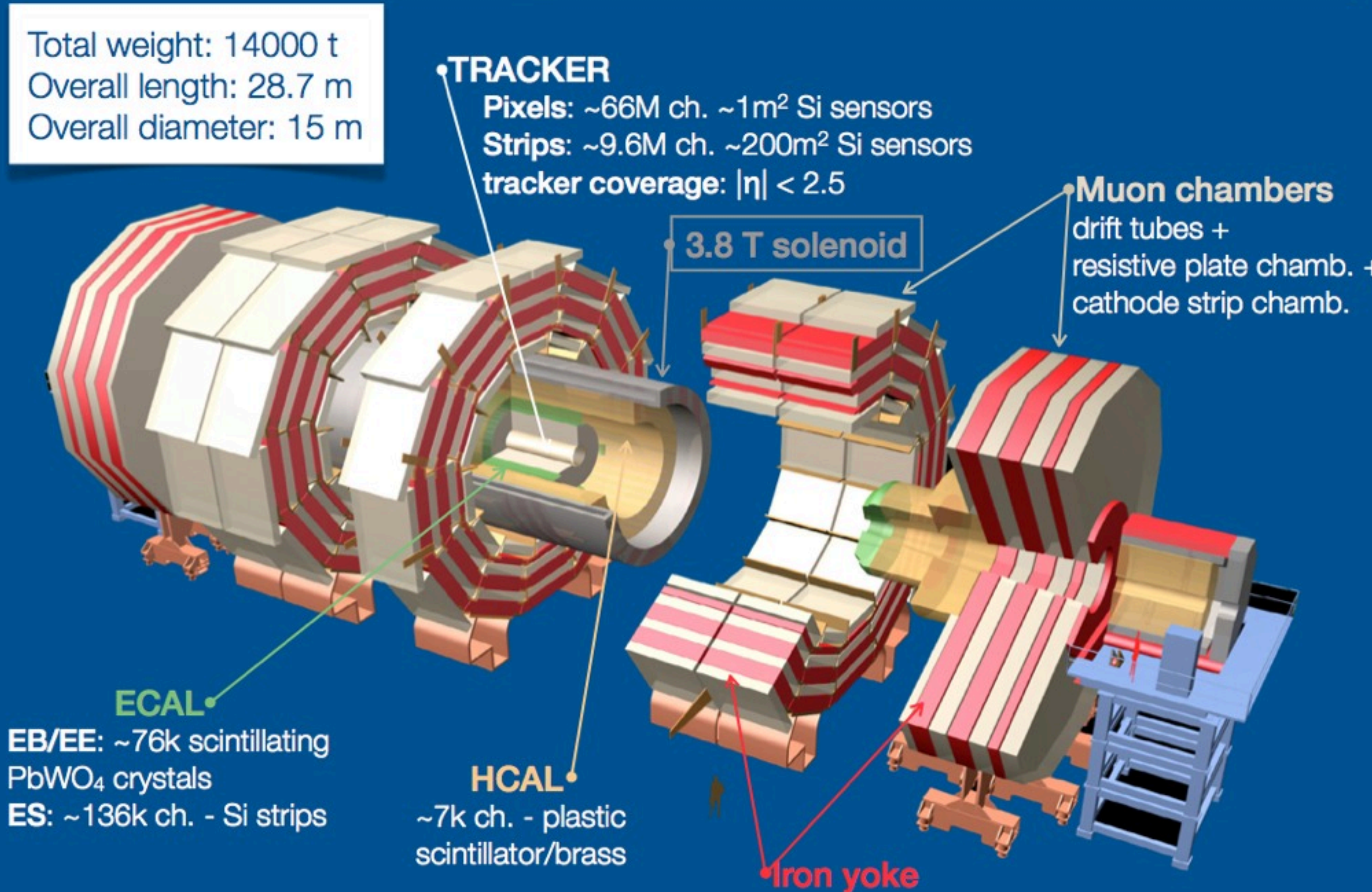

Crystals and photodetector

- $PbWO_4$
  - high density to allow a compact calorimeter ($\rho = 8.3$ g/cm^3)
  - short radiation length ($X_0 = 0.89$ cm ⇒ a crystal is about 25 X_0)
  - small Molière radius ($r_M = 2.2$ cm)
  - low light yield (LY) / fast emission (~30 γ/MeV, 80% within 25 ns)
  - **LY spread** between crystals **~10%**
  - **LY variation** with **temperature: -2.2%/°C**
  - **transparency variation with radiation**

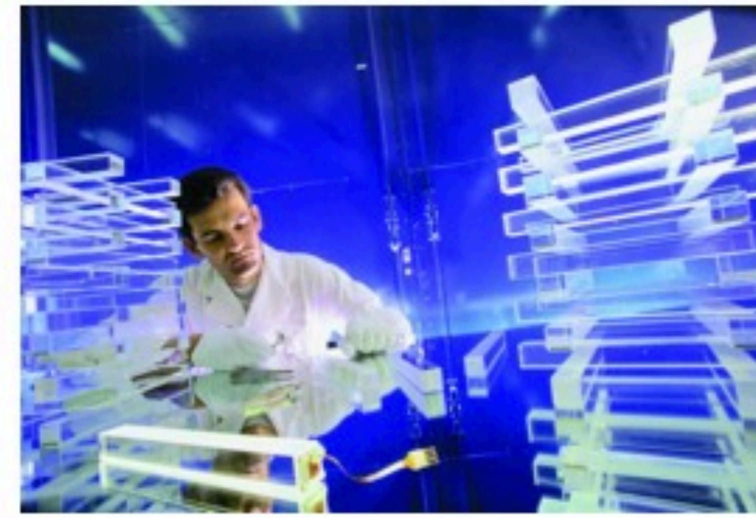

- **Barrel photo-detectors: Avalanche Photo Diodes**
  - two APDs of 5x5 mm^2 per crystal: ~4.5 p.e./MeV
  - nominal gain: 50
  - gain variation: $\Delta G/\Delta T$ **= -2.4%/°C**, $\Delta G/\Delta V$ **= 3.1%/V**

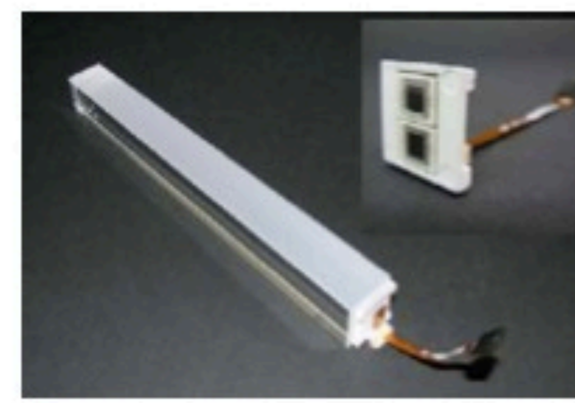

- **Endcap photo-detectors: Vacuum Photo Triodes**
  - one VPT of ~280 mm^2 per crystal: ~4.5 p.e./MeV
  - **gain spread** among VPTs **~25%**

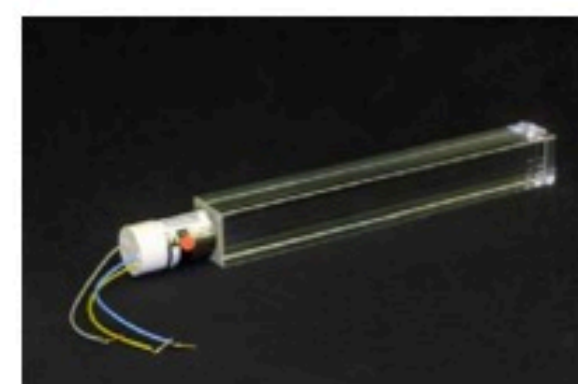

Z→μμγ

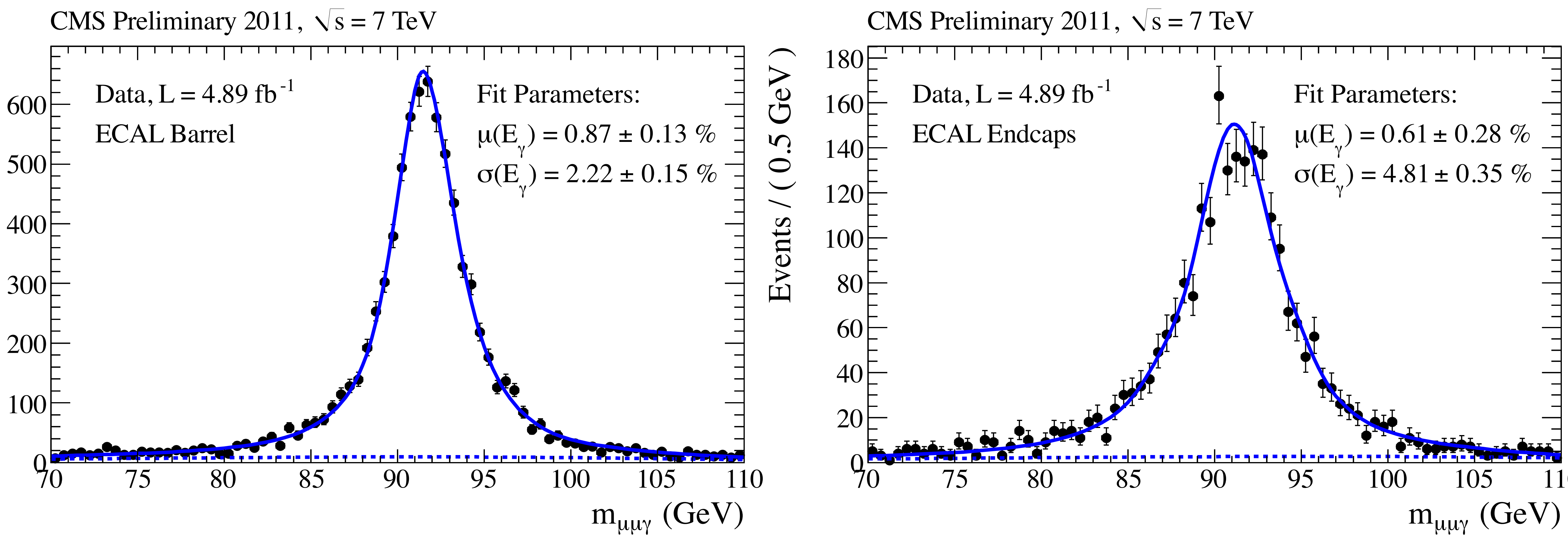

- Invariant mass distribution of Z→μμγ final states from 2011 DATA. The photon energy scale and resolution are extracted from de-convoluting the Z line shape in this final state. The inclusive categories are shown.

- The energy scale and resolution are in agreement with the values measured for electrons from Z->ee decays.

E/p template method

- The *E/p* **variable** can be used to study the **ECAL relative energy scale**
  - *E* is the electron energy as measured by **ECAL**
  - *p* is the electron momentum as measured by the **tracker**

E/p **~1** for non-showering, well reconstructed electrons

- Implicitly assuming that all instabilities arise from *E*
  - ad-hoc momentum calibration applied in specific cases (e.g. studies vs. η)

- Build an *E/p* **template distribution** *T* from data and **fit** it to a **subset** of the same data, **scaling** *E* **of a factor κ**

$$f(E/p) = N \cdot \kappa \cdot T(\kappa E/p)$$

- **1/κ ⇒ relative scale** of the subset w.r.t. the template

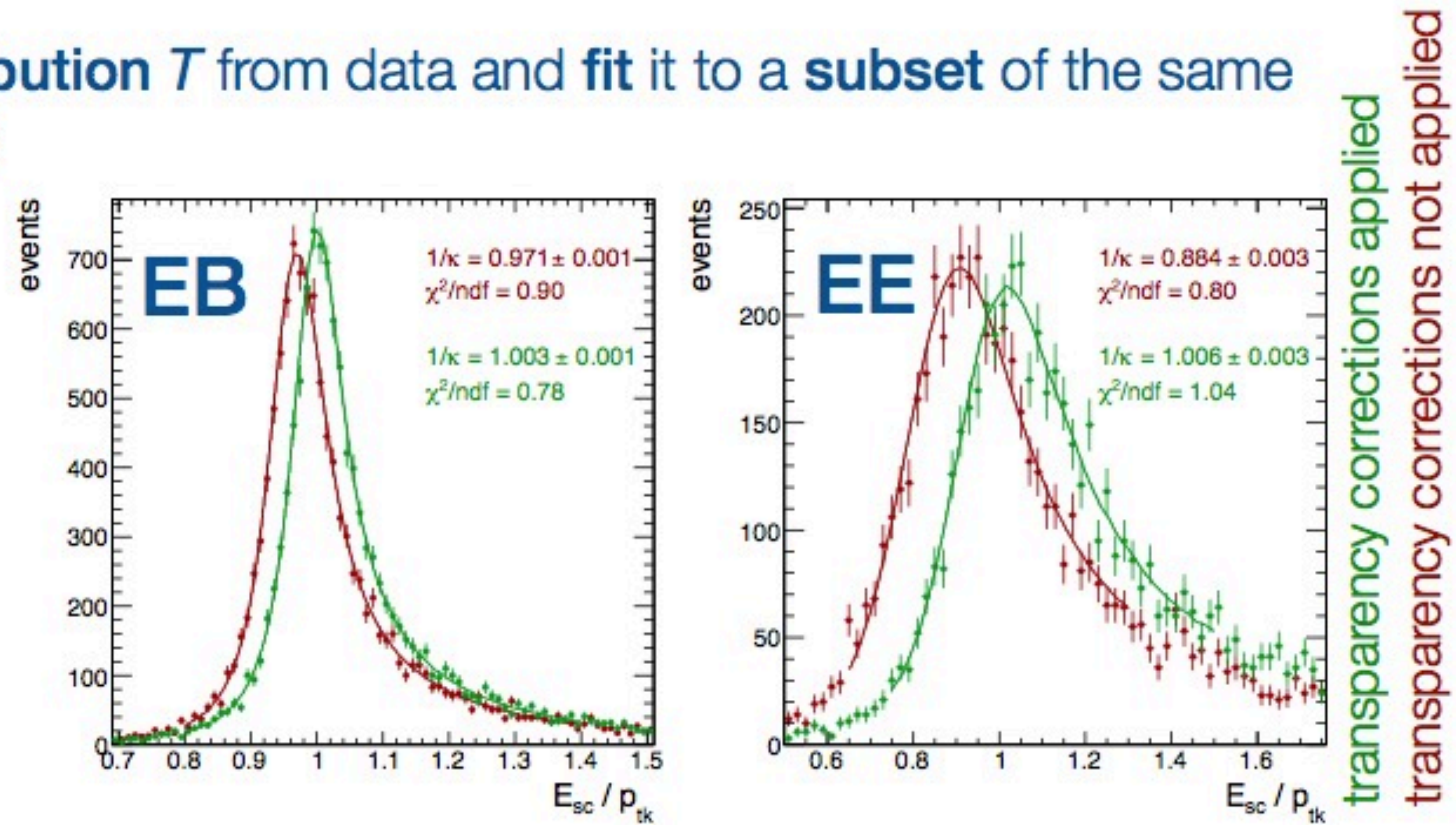

Impact of the clustering on the Z→ee

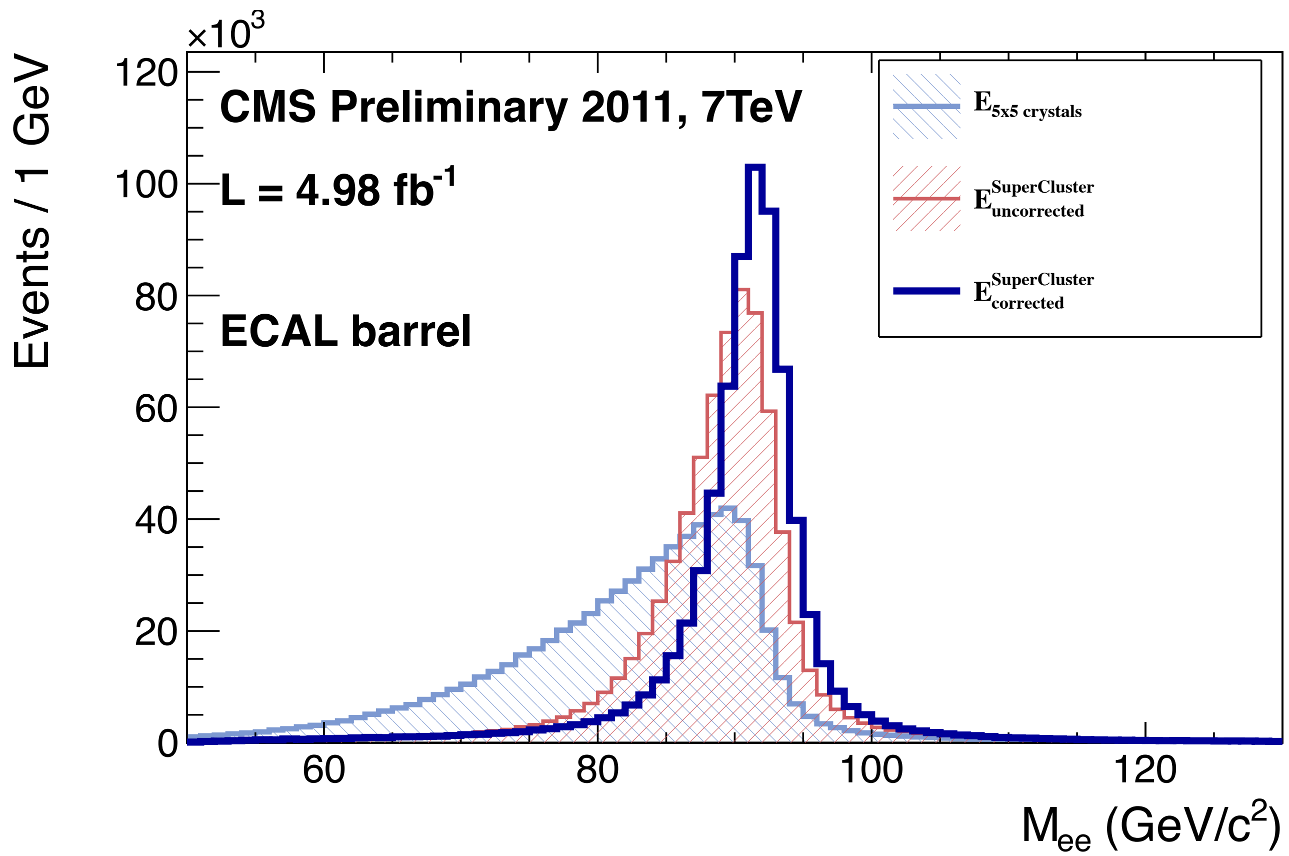

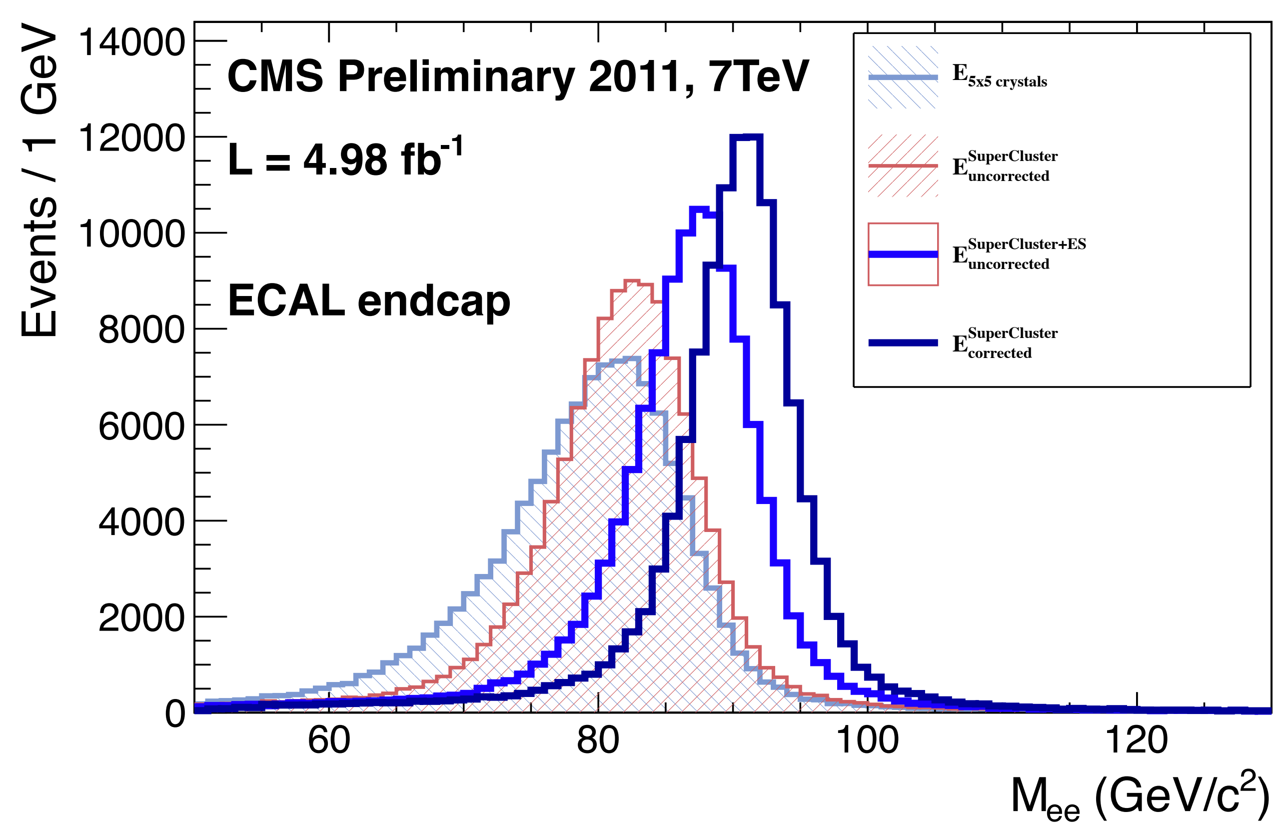

- The plots show the impact on the Z→ee energy scale and resolution from the incorporation of more sophisticated clustering and cluster correction algorithms.

H→γγ backgrounds

- Irreducible background is dominant:
  - **70% from 2 prompt photons**

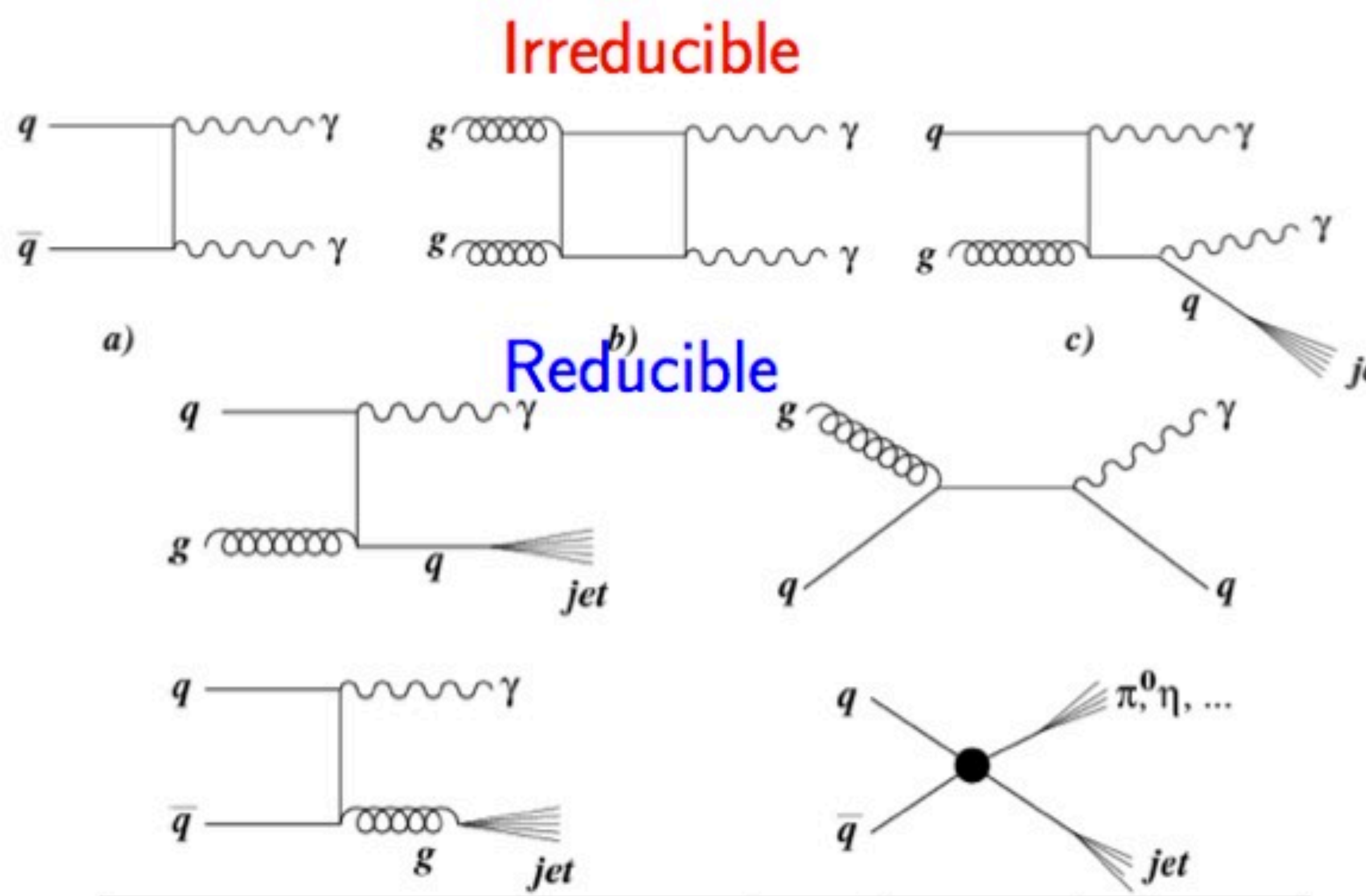

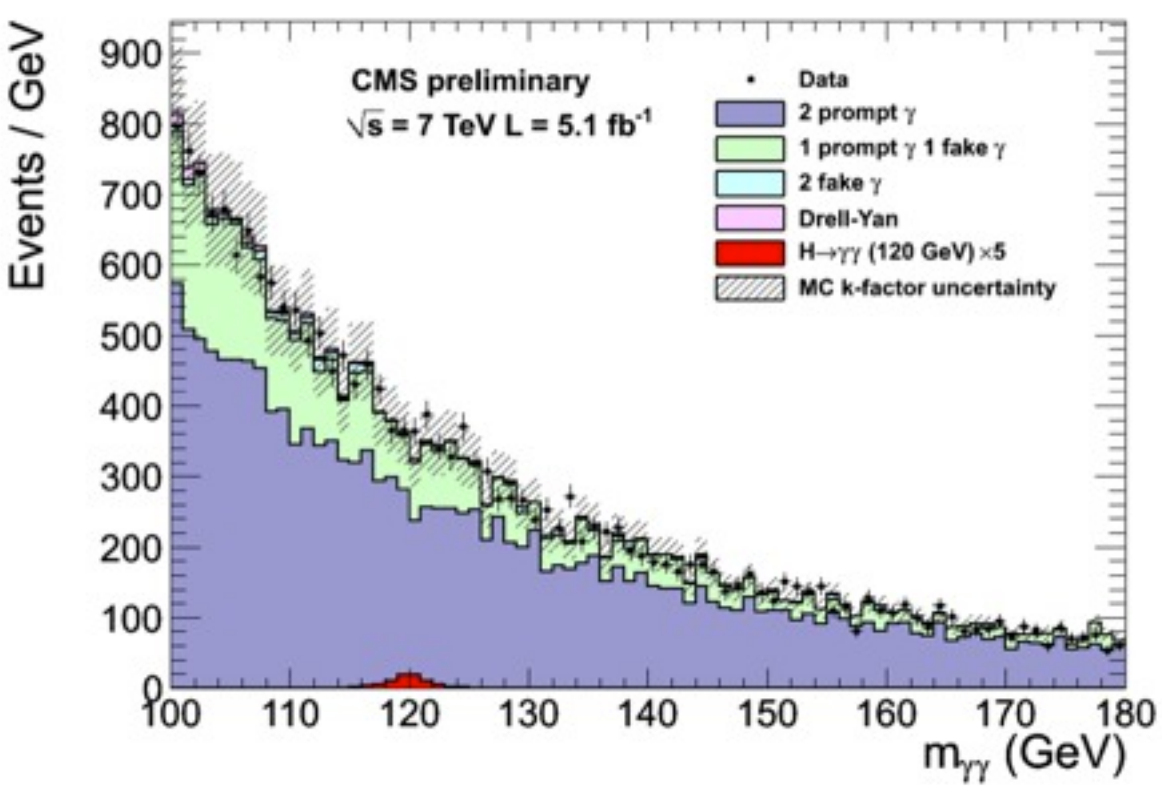

Process	p_T (GeV)	σ_{LO} (pb)
$H \to \gamma\gamma$ (120 GeV)	–	0.044 (NNLO)
pp→ $\gamma\gamma$ (Born)	> 25	22.4
pp→ $\gamma\gamma$ (Box)	> 25	12.4
pp→ γ+jet	> 30	2.0×10^4
pp→jets	> 30	6.0×10^7
Drell Yan ee	–	3×10^3

MVA categories

- Class boundaries **optimized to give the best expected limit** using MC background

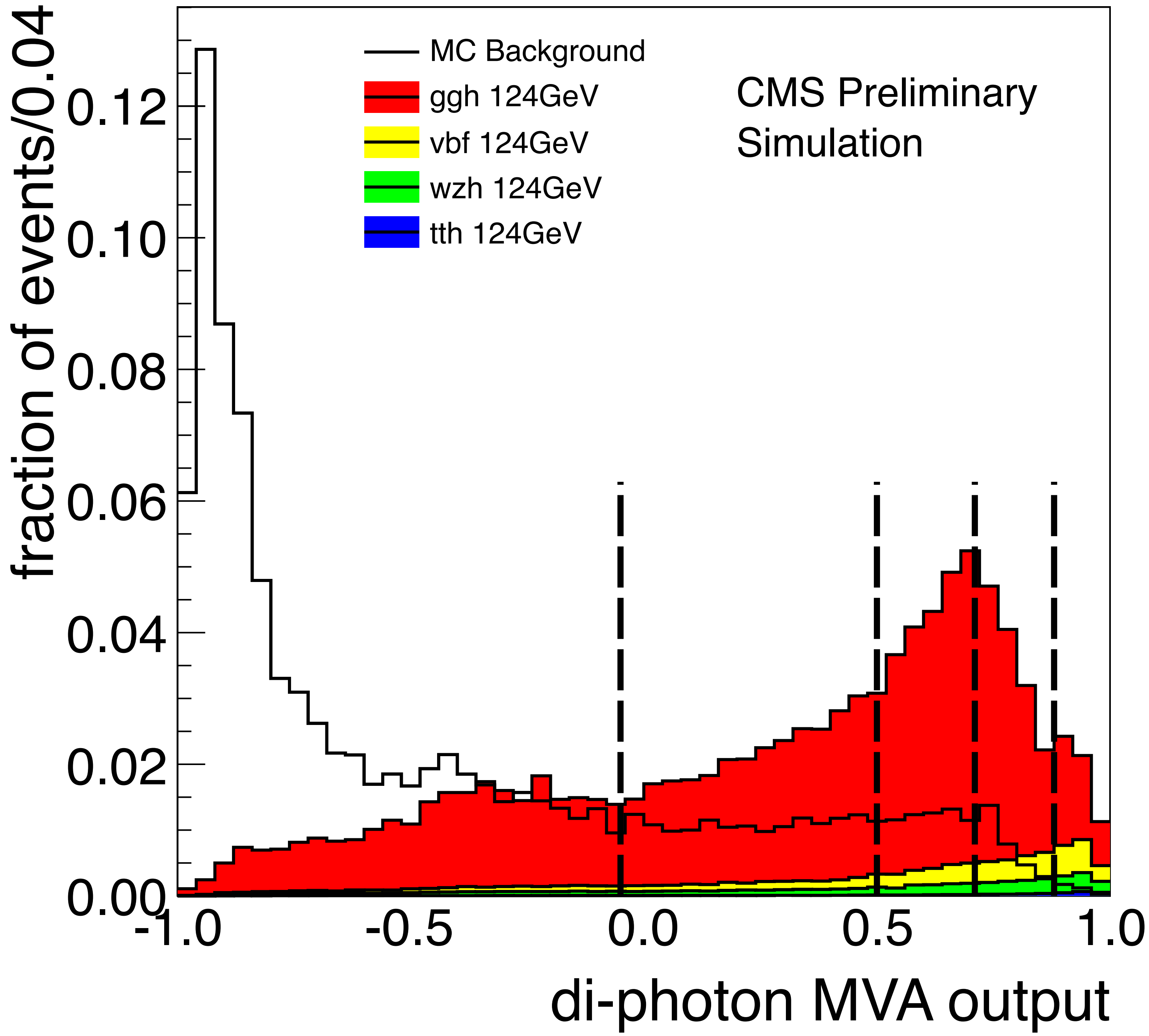

Combined 2011+2012 H→γγ results

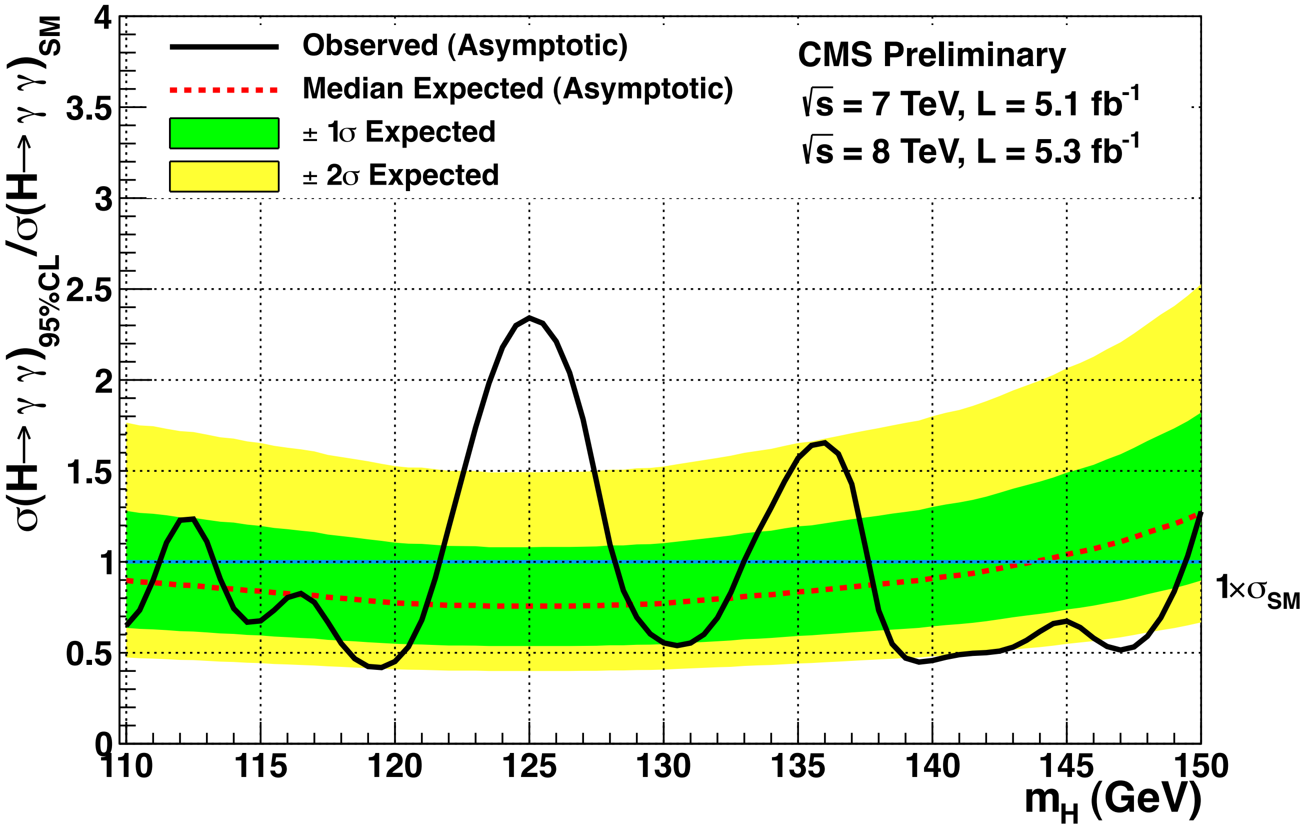

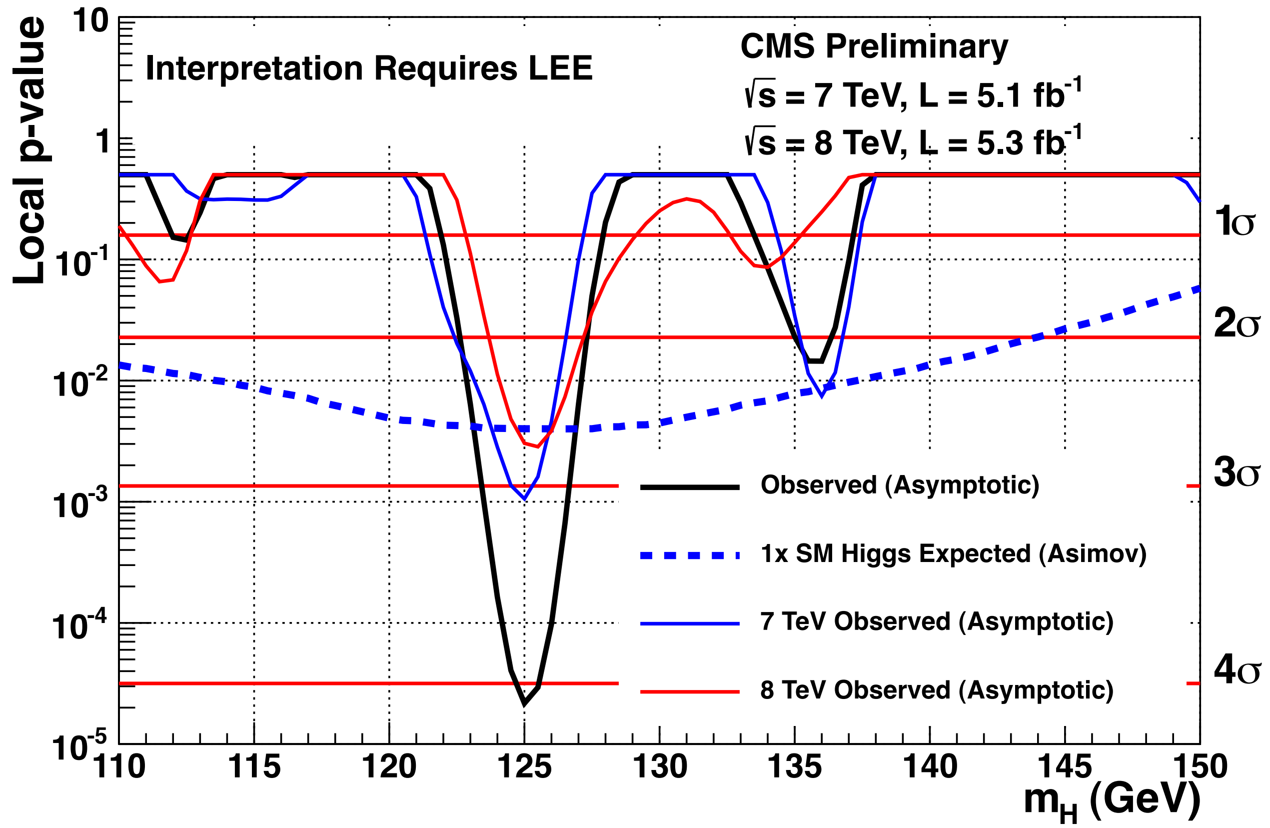

- Exclude the SM Higgs at 95% CL: 114–121, 129–132, 138–149 GeV
- Observed excess consistent with narrow resonance around 125 GeV mass at 4.1σ